Copyright Warning & Restrictions

The copyright law of the United States (Title 17, United States Code) governs the making of photocopies or other reproductions of copyrighted material.

Under certain conditions specified in the law, libraries and archives are authorized to furnish a photocopy or other reproduction. One of these specified conditions is that the photocopy or reproduction is not to be "used for any purpose other than private study, scholarship, or research." If a, user makes a request for, or later uses, a photocopy or reproduction for purposes in excess of "fair use" that user may be liable for copyright infringement,

This institution reserves the right to refuse to accept a copying order if, in its judgment, fulfillment of the order would involve violation of copyright law.

Please Note: The author retains the copyright while the New Jersey Institute of Technology reserves the right to distribute this thesis or dissertation

Printing note: If you do not wish to print this page, then select "Pages from: first page # to: last page #" on the print dialog screen

NJIT New Jersey's Science & Technology University

The Van Houten library has removed some of the personal information and all signatures from the approval page and biographical sketches of theses and dissertations in order to protect the identity of NJIT graduates and faculty.

INFORMATION TO USERS

This material was produced from a microfilm copy of the original document. While the most advanced technological means to photograph and reproduce this document have been used, the quality is heavily dependent upon the quality of the original submitted.

The following explanation of techniques is provided to help you understand markings or patterns which may appear on this reproduction.

1. The sign or "target" for pages apparently lacking from the document photographed is "Missing Page(s)". If it was possible to obtain the missing page(s) or section, they are spliced into the film along with adjacent pages. This may have necessitated cutting thru an image and duplicating adjacent pages to insure you complete continuity.

2. When an image on the film is obliterated with a large round black mark, it is an indication that the photographer suspected that the copy may have moved during exposure and thus cause a blurred image. You will find a good image of the page in the adjacent frame.

3. When a map, drawing or chart, etc., was part of the material being photographed the photographer followed a definite method in "sectioning" the material. It is customary to begin photoing at the upper left hand corner of a large sheet and to continue photoing from left to right in equal sections with a small overlap. If necessary, sectioning is continued again — beginning below the first row and continuing on until complete.

4. The majority of users indicate that the textual content is of greatest value, however, a somewhat higher quality reproduction could be made from "photographs" if essential to the understanding of the dissertation. Silver prints of "photographs" may be ordered at additional charge by writing the Order Department, giving the catalog number, title, author and specific pages you wish reproduced.

5. PLEASE NOTE: Some pages may have indistinct print. Filmed as received.

Xerox University Microfilms
300 North Zeeb Road
Ann Arbor, Michigan 48106

73-27,030

WANG, Huei-hsiung, 1944-
REPRESENTATION AND CHARACTERIZATION OF
THIXOTROPIC FLUIDS.

Newark College of Engineering, D.Eng.Sc., 1973
Engineering, chemical

University Microfilms, A XEROX Company, Ann Arbor, Michigan

REPRESENTATION AND CHARACTERIZATION OF THIXOTROPIC FLUIDS

BY

HUEI-HSIUNG WANG

A DISSERTATION

PRESENTED IN PARTIAL FULFILLMENT OF

THE REQUIREMENTS FOR THE DEGREE

OF

DOCTOR OF ENGINEERING SCIENCE

AT

NEWARK COLLEGE OF ENGINEERING

This dissertation is to be used with due regard to the rights of the author. Bibliographical references may be noted, but passages must not be copied without permission of the College and without credit being given in subsequent written or published work.

Newark, New Jersey

1973

ABSTRACT

Thixotropy is a time-dependent rheological behavior of a group of fluids which are characterized by an isothermal reversible breakdown induced by a mechanical disturbance. Based on this definition, a mathematical model of reversible degradation kinetics is set up. Its development leads to two equations which represent quantitatively the hysteresis loop and torque-decay curve. These equations consist of five independent parameters with their physical meanings. These parameters can be used to characterize the properties of thixotropic materials.

The original Weissenberg Rheogoniometer was modified to measure the thixotropic behavior of blood with the step change and the ramboid change of shear rate. The results of experimental measurements confirmed that blood is a thixotropic material. This is explained by the breakdown of rouleaus and clumps as an aggregated form of erythrocytes into single red cells as a non-aggregated form of erythrocytes.

The comparison of model prediction with the experimental results shows that the model equations can quantitatively represent the behavior of bloods. Therefore the parameters determined by the experimental data are used to compare and characterize the physical-chemical properties of blood.

APPROVAL OF DISSERTATION

REPRESENTATION AND CHARACTERIZATION

OF THIXOTROPIC FLUIDS

BY

HUEI-HSIUNG WANG

FOR

DEPARTMENT OF CHEMICAL ENGINEERING

NEWARK COLLEGE OF ENGINEERING

BY

FACULTY COMMITTEE

APPROVED: _____ CHAIRMAN

_____

_____

_____

_____

NEWARK, NEW JERSEY

June, 1973

ACKNOWLEDGEMENTS

The author acknowledges the encouragement, advice and guidance offered by Dr. C. R. Huang throughout this investigation. The author thanks Dr. Siskovic for his assistance in construction of the experimental apparatus.

The author acknowldeges the financial support of this work by the National Science Foundation (Grant GK-4689), and by the Newark College of Engineering Research Foundation. In addition, the author offers special thanks to his wife, Chuen-Meei, for her understanding, patience and confidence; and to his parents for their inspiration.

TABLE OF CONTENTS

TABLE OF CONTENTS (continued)

LIST OF FIGURES

LIST OF TABLES

LIST OF TABLES (continued)

INTRODUCTION

Thixotropy

As early as 1935, Freundlich (1) found a concentrated clay suspension which "gels" on quiet standing and "liquifies" upon agitation, and introduced the term "thixotropy" (thixis means stirring or shaking; trepi means turning or changing) to describe the behavior of reversible isothermal gel-sol-gel transformation disturbed by mechanical agitation and subsequent rest. Since then, a large group of materials such as paint (2), printing ink (3), and products of food industries have been found to have the thixotropic properties. Thixotropy becomes a very common type of rheological phenomenon and important in industrial studies.

In the forties, the extensive investigation on thixotropic materials were carried out by Green and Weltmann (6-10). In their work, a rotational Couette type viscometer (43) was used to generate a flow curve by linearly increasing the rate of shear to a predetermined point and then decreasing the rate of shear to zero. If thixotropy exists in the testing material, a hysteresis loop would be found in the flow curve. Therefore they claimed that the hysteresis loop gave the information closely analogous to that

obtained from measurement of "setting time" and similar to "largest setting time"; the biggest "hysteresis loop" said t, be more thixotropic.

Although the term "thixotropy" had been introduced, the original definition of Freundlich was not uniformly adhered to. Various investigators (20,49,56,67) intended to re-define thixotropy in terms of rheological concepts, independent of the "gel-sol-gel" description, but they did not agree with each other. Recently the Joint Committee on Rheology of the International Council of Scientific Unions (12) has made the following definition of thixotropy:

> A thixotropic system exhibits a time dependent, reversible, and isothermal decrease of viscosity with shear in flow.

This definition omits the "gel-sol-gel transformation" as had in Freundlich, but contains the restriction of time-dependence which could be itself limited by the speed of measurement (4). These are some characteristics from the current accepted definition (29):

1. It accompanies an isothermal change which is brought about by applying a mechanical disturbance to a system.
2. When the mechanical disturbance is removed, the system

recovers its original structure.

3. The flow curve of the system has a hysteresis loop.

General Description of Rheology

Rheology is a science of flow and deformation of matter (13,5). Flow and deformation are the results of movement of particles of a body, relating to one another. Materials under forces are deformed either elastically, if the deformation reaches a definite state under the action of finite forces, which goes back when the forces are removed; plastically, if the deformation remains permanent when the forces are removed; flows, if under the action of finite forces, the deformations continuously increase without limit; or viscoelastically, if material shows both elastic and flow behavior.

In studying the transport of material from one place to another, we see there exists some relationship between the shear stress, τ, the dynamical variable at some instant and the shear rate, $\dot{r}$, the kinematical variable at some instant, or the kinematical state of the system at all instants of the past. The equation expressing the relation between dynamical and kinematical variables is called rheological equation of state, or constitutive equation. The rheological equation of state can be used to classify viscous fluid. There are two main fluids (11); Newtonian and non-Newtonian fluid.

Newtonian Fluid-the Ideal Fluid

Newtonian fluids are those fluids exhibiting a direct proportionality between shear stress and shear rate in laminar flow, as proposed by Newton. Mathematically, it can be expressed as

$$\tau = \mu \dot{r} \qquad (1\text{-}1)$$

where τ is the shear stress, $\dot{r}$ is the rate of shear, and μ is the viscosity, which is effected only by temperature and pressure for a given system.

As shown in Figure (1-1), the flow curve (a plot of shear stress versus shear rate) of Newtonian fluid is a straight line with a slope equal to the viscosity.

Non-Newtonian Fluid

There are many real materials, particularly polymer melts, solutions, and the suspension of particles in liquids such as blood, for which the shear stress is not linearly related to the shear rate. They are called non-Newtonian. This fluid unlike Newtonian can not possess a constant coefficient of viscosity at a given temperature and pressure (Figure 1-1). The values calculated from the ratio of the applied shear stress to the shear rate are called apparent viscosity.

Non-Newtonian fluid can also be classified into three broad classes of flow behavior (14); time-independent, time-dependent, and elastico-viscous fluids.

Figure 1-1

Shear Stress-Shear Rate Relation for Newtonian and non-Newtonian Fluids

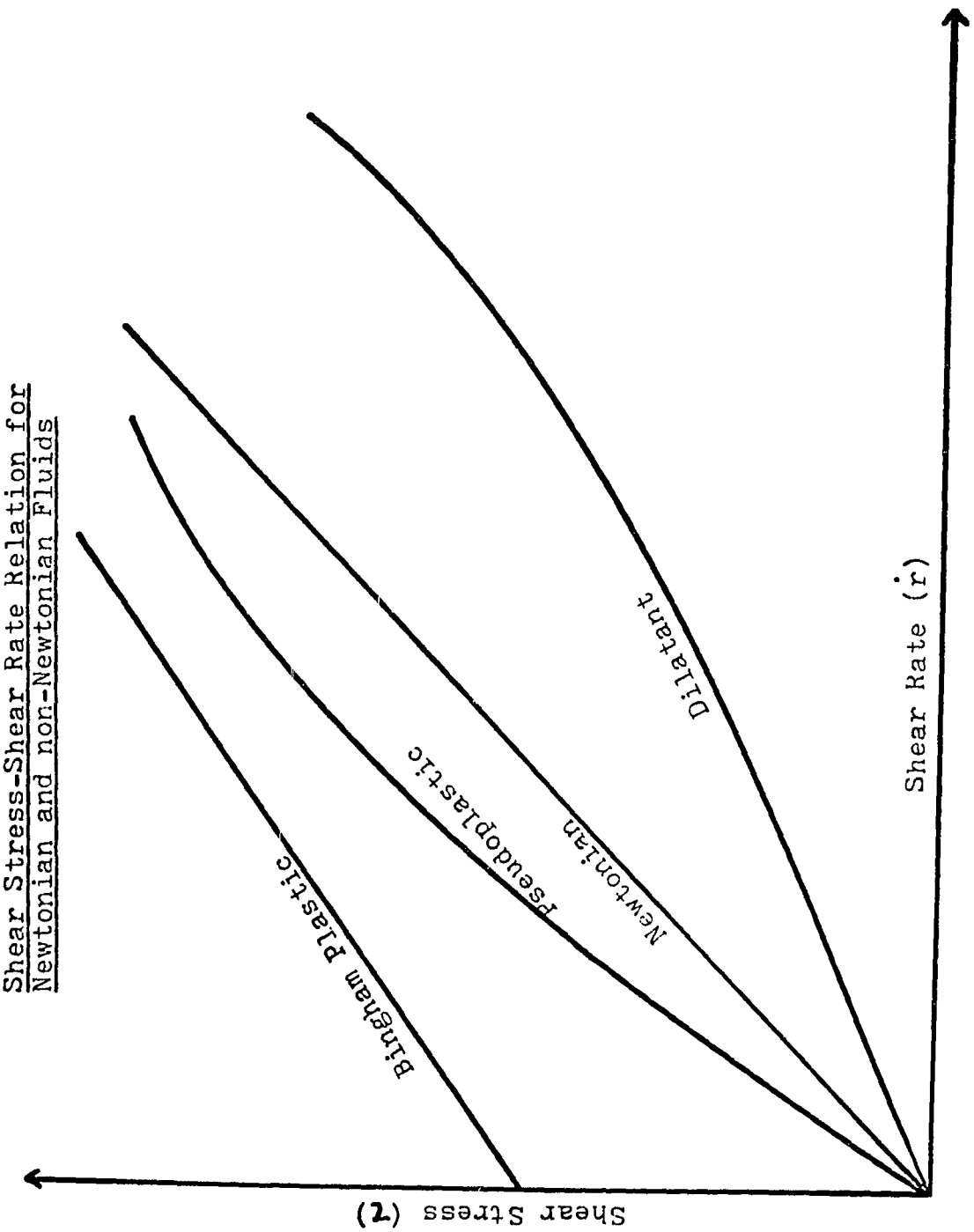

Time-independent Fluid

Time-independent fluids are those in which shear rate at a given point is solely a function of shear stress at that point and nothing else. Pseudoplastic, Bingham and dilatant fluids fall into this category.

Psedoplastic fluid, as observed in most polymer solution, is a shear thinning material, i.e., the viscosity decreases as the rate of shear is increased. The flow curve of this material is shown in Figure 1-1, which is nonlinear, concave downward.

The opposite behavior to pseudoplastic is known as dilatant. Dilatant materials show an increase in the apparent viscosity with increasing shear rate (Figure 1-1). Dilatancy is often observed in highly concentrated suspensions, such as sand or PVC paste.

The Power law or Ostwald-de Waele equation is the simplest and useful rheological equation to describe pseudoplastic and dilatant behaviors. The equation takes the form as

$$\tau = k(\dot{r})^n = \mu_a \dot{r} \qquad (1\text{-}2)$$

or

$$\tau = k(\dot{r})^{n-1} \qquad (1\text{-}3)$$

where k is a constant and μ_a is apparent viscosity of Power-law fluids.

In equation (1-3), if n less than one, the apparent viscosity, μ_a, is decreasing with the increase of shear rate, therefore it is pseudoplastic; if n greater than one, the fluid will be dilatant; if n equals to one, the equation is reduced to equation (1-1) and it is Newtonian.

Bingham plastic is another kind of time-independent fluid, in which it remains rigid when shear stress is of smaller magnitude than the yield stress τ_y, but flows somewhat like a Newtonian fluid when the shear stress exceeds the yield value (Figure 1-1), i.e.,

$$\tau = \tau_y + \mu \dot{r} \qquad (1-4)$$

where τ_y is yield stress.

A number of suspensions, slurries and pulps approximate in their behavior to Bingham plastic although the stress and shear rate relationship is not so straight above yield value.

Elsatico-viscous Fluids

Elastico-viscous fluids are those which show predominantly viscous but exhibit partial elastic

recovery after deformation, in other words, the material may be outwardly liquid and capable of indefinite deformation but on release of the deforming stress show some recovery of shape (14,73).

The quantitative description of an elastico-viscous fluid was first obtained by refering it to a simple idealized model which considers the material to be a combination of a spring and dashpot in series (Maxwell model). The spring is stipulated to show linear elastic behavior and the dashpot to have Newtonian characteristics. With this approach, the model gave an introduction to the mathematical description of an elastico-viscous material and induced a generalized rheological equation for a linear visco-elastic material.

$$P'\tau^{ij}(x,t)=2D'\dot{r}^{ij}(x,t) \qquad (1\text{-}5)$$

where P' and D' are the linear operators,

$$P'=1+\lambda\frac{\partial}{\partial t}+\lambda_1\frac{\partial^2}{\partial t^2}+\cdots+\lambda_N\frac{\partial^{N+1}}{\partial t^{N+1}}$$
$$D'=\mu_0\left(1+\eta\frac{\partial}{\partial t}+\eta_1\frac{\partial^2}{\partial^2 t}+\cdots+\eta_M\frac{\partial^{N+1}}{\partial t^{N+1}}\right)$$

where μ_0 is the viscosity of the material at zero rate of shear, and the parameters $\lambda_0, \lambda_1, \cdots, \lambda_N, \eta_0, \eta_1, \cdots, \eta_M$ are supposed to be properties of the material.

As indicated in equation (1-5), the shear rate in elastico-viscous liquid is a function of shear stress and strain, as well as their time derivatives.

The rheological behavior of elastico-viscous material usually manifests itself in such phenomena as die swell, calender swell, neck-in, and frozen-in orientations.

Time-dependent Fluid

Time-dependent fluids are those in which shear rate is a function of both shear stress and time, $\dot{r}=F(\tau,t)$. There are three kinds of time-dependent fluids; thixotropic, anti-thixotropic, and rheopectic (4,14).

Thixotropy, as we pointed out previously, is a reversible structure breakdown as mechanical agitation is applied. The materials are commonly observed in systems like emulsions, suspensions, organic and inorganic solutions at high concentration.

Anti-thixotropy is considered to be an opposite to thixotropy. It is an increase of viscosity during the flow. Once again, a hysteresis loop is produced in the rotational viscometer experiment, but in an opposite sense of the thixotropic loop. The anti-thixotropic fluids can be found in gypsum paste, in water or ammonium oleate suspensions.

Rheopexy is considered as the same meaning as anti-thixotropy, an opposite to thixotropy (4, 81), although some investigators did not agree to that (16). A thixotropic material breaks down under a shear rate, whereas a rheopectic material builds up with a shear.

Measurements of Thixotropy

A variety of experimental techniques of measuring the characteristics of thixotropic fluid have been proposed by various investigators (6,9,76-80). If shear rate is the variable to be controlled in the rheological measurement, as frequently used, there are three kinds of shear rate variations in the input system: step change, ramboid change, and trapezoid change of shear rate.

1. Step change of shear rate

As shown in Figure (1-2), at the begining a selected constant shear rate, $\dot{r}_o$, is maintained for a time sufficiently long until an equilibrium shear stress is reached, then a greater shear rate $\dot{r}$ (or a smaller shear rate) is applied. The shear stress is measured and shown as a function of chosen shear rate and time, $\tau = F(\dot{r}_o, \dot{r}, t)$. Eventually the shear stress will reach an equilibrium value and become independent of time of shearing. As shown in Figure (1-2), the equilibrium magnitude of torque-decay curve (a plot of

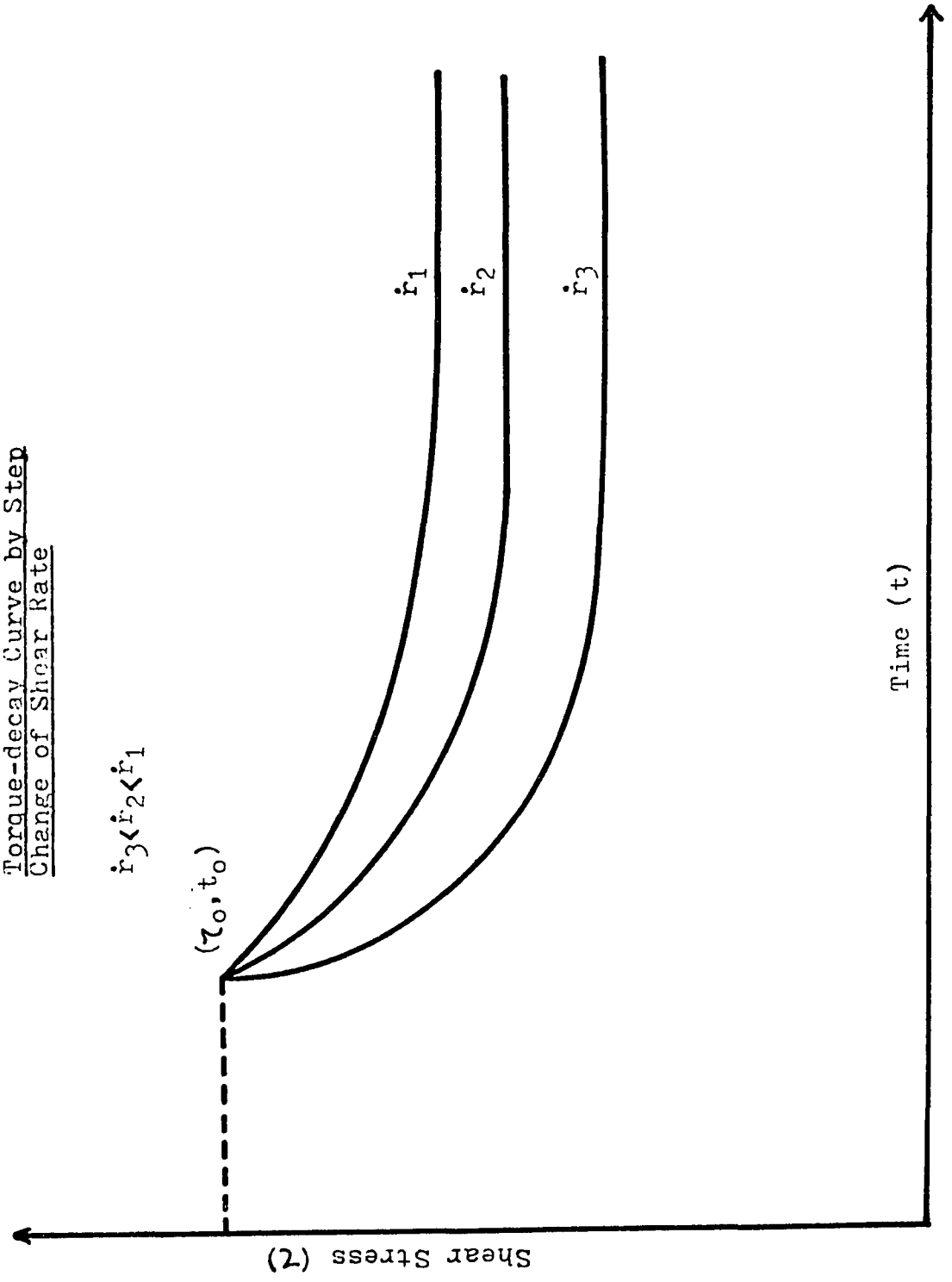

Figure 1-2

Torque-decay Curve by Step Change of Shear Rate

shear stress versus time) depends on the shear rate applied. The greater the shear rate being applied, the greater the shear stress of the material will be obtained.

2. Ramboid change of shear rate

A time-dependent fluid is subjected to a constant shear rate, $\dot{r}_o$, until a state of equilibrium is reached. Then the applied shear rate is linearly increased to a predetermined value and then immediately decreased toward initial shear rate in the similar manner. The shear stress is measured and shown as a function of both shear rate and time, $\tau = G(\dot{r}_o, \dot{r}, t)$. When the shear rate is returned to the original value $\dot{r}_o$, a hysteresis loop will be obtained. The size of the loop will depend on the thixotropic property of the material, the rate of increase of shear rate and the maximum shear rate applied. The flow curve for an ideal material is shown in Figure (1-3). If the second loop of shear rate is immediately started right after the completion of first run, the loop would not be the same. The shear stress for this loop will be lower at the same value of shear rate, and the area in this loop will be smaller. If still repeating the same process again and again, the area of hysteresis loop will gradually decrease until an equilibrium state is reached. At this time, the material behaves like a pseudoplastic in which the shear

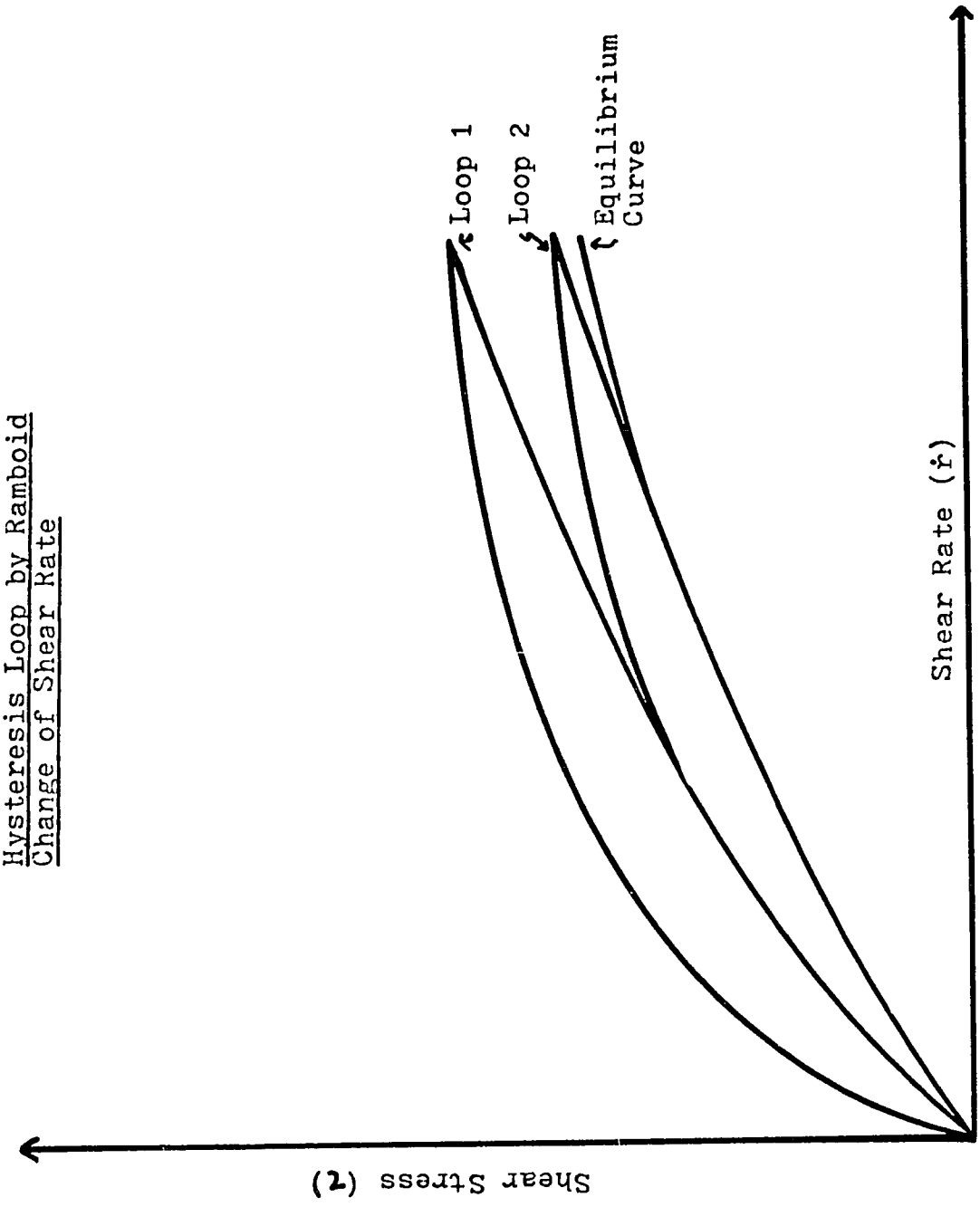

Figure 1-3

Hysteresis Loop by Ramboid Change of Shear Rate

stress is dependent only on shear rate but not on time.

3. Trapezoid change of shear rate

Initially it is the same procedure as it was in ramboid change of shear rate. But when the maximum shear rate is reached, the shear rate $\dot{r}_m$ is maintained. At this moment, the material under the shear rate will reduce its shear stress until a limiting shear stress is reached. Then in the remaining cycle the shear rate is linearly decreasing and returns to original value. A hysteresis loop is also obtained in trapezoid change of shear rate as shown in Figure (1-4).

It is important to mention that the area and the shape of hysteresis loop in ramboid or trapezoid change of shear rate is dependent on the rate of increase and the rate of decrease of shear rate in the cycles. If the rate of change of shear rate in the parts of a cycle were so extremely slow that equilibrium continually was reached between breakdown and build-up processes, a limiting equilibrium flow curve would be approached, with a vanishing loop area. Since both the thixotropic properties of the material and the rate of change of shear rate are the major factor in determining the size of the area enclosed in the flow curve loop, a material showing the largest area in the cycle with similar controlled shear rate variation may be said to be more thixotropic, which was indicated by Green and Weltmann.

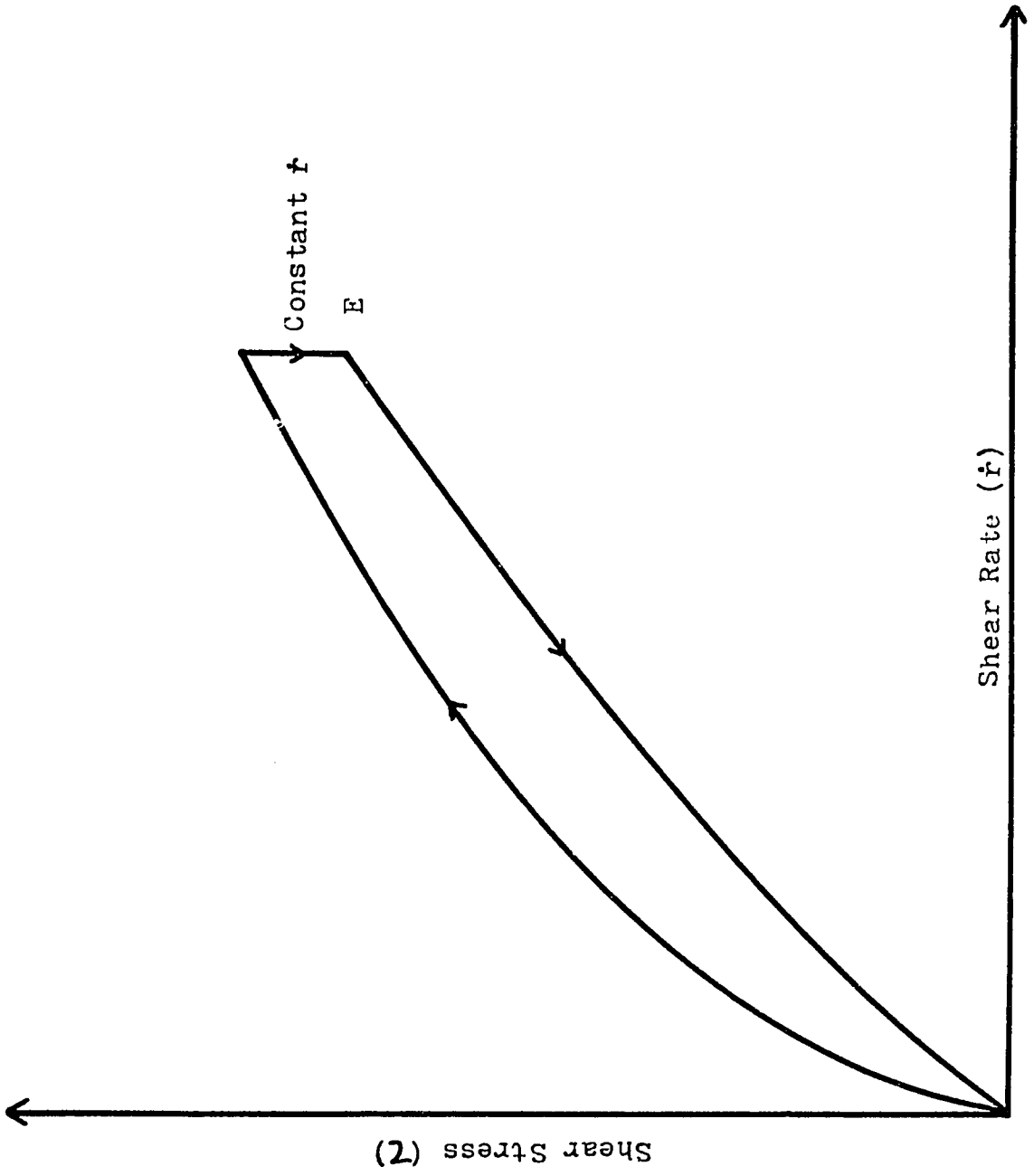

Figure 1-4

Hysteresis Loop by Trapezoid Change of Shear Rate

The objective of this theses is to derive a rheological equation based on a mathematical model of reversible degradation kinetics for the thixotropic material. This equation can represent quantitatively the torque-decay curve, the hysteresis loop, and other flow curves which are the different combinations of these two curves. The human blood, which is considered as a time-independent (60,48) or a time-dependent, (not necessarily thixotropic (63)) is measured by applying a step change or a ramboid change of shear rate. If the blood is thixotropic, both hysteresis loop and torque-decay curve will be obtained. From the experimental data of these measurements, the parameters in the rheological equation which have their physical meanings were determined and used to represent all these characteristics of the rheological behavior of a thixotropic fluid.

REVIEW OF PREVIOUS WORK

In this chapter we intend to review some approaches which have been done by several investigators and the rheological background of blood, a time-dependent fluid which is going to be used in the experiment.

Previous Approaches

Various approaches have been attempted to interpret or to correlate the complicated rheological behavior of thixotropic fluids. Based on the different approaches, three major branches may be classified. There are empirical, modeling, and functional analysis approaches.

Empirical Approach

In this approach, empirical data were taken in the region of interest and an empirical equation is obtained based on these data. Green and Weltmann (6-9,27) first did a series of experimental work by using a rotational viscometer. Instead of only studying the upward portion of flow curve (Figure 2-1) as other investigators did (20,21), they considered the whole hysteresis loop as a measure of thixotropy and defined "degree of thixotropy" to distinguish the intensity of each thixotropic material. Quantitatively they (8,17) defined the plastic viscosity U as the excess shear stress (with respect to yield value) for inducing unit rate of shear or from Figure (2-1)

$$U=(\tau_2-\tau_1)/\dot{\gamma}_c \qquad (2\text{-}1)$$

Figure 2-1

Hysteresis Loops of Continuous Ramboid Change of Shear Rate

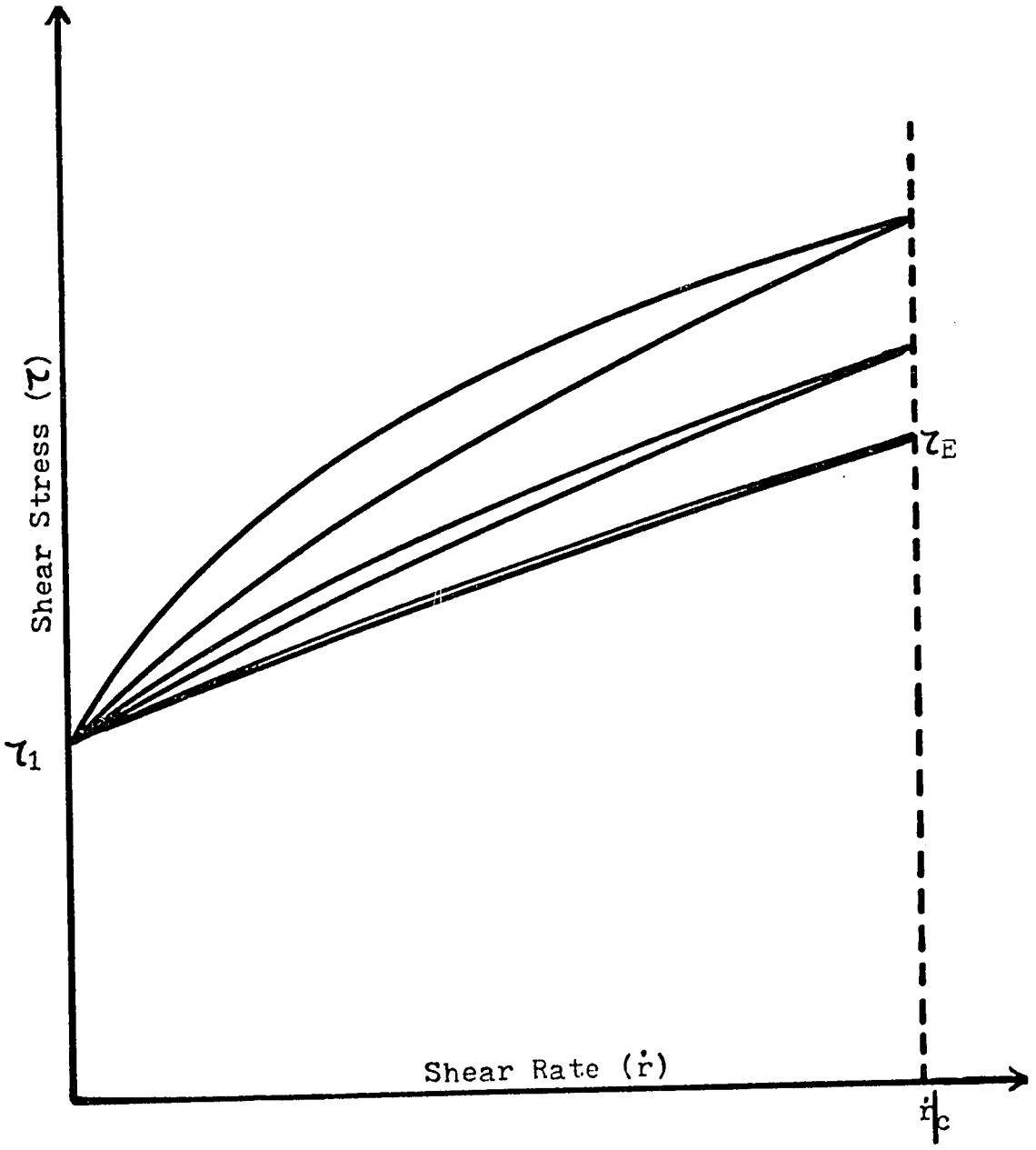

and also from the experiment work they found out that the relationship between the plastic viscosity and time is

$$\exp\left[-(U_1-U_2)/B\right]=t_1/t_2 \qquad (2\text{-}2)$$

where U_1 and U_2 are the plastic viscosity measured at t_1 and t_2, B is proportionality.

Rearranging equation (2-2), the time coefficient of thixotropic breakdown, B, can be expressed as

$$B=(U_1-U_2)/\ln(t_2-t_1) \qquad (2\text{-}3)$$

The numerical value of B could be obtained experimentally from a series of hysteresis loops and might be considered as a constant to specify the thixotropic fluid.

One of the most important contribution from their approach is that they distinguished two variables, rate of shear and time, since both effect the structure breakdown.

Dahlgren (18) refined the analytic treatment of thixotropic breakdown based on the experimental work of Green and Weltmann. He found the plastic viscosity is a function of shear rate as

$$dU=-M\left[d(\tau/\dot{r})\right] \qquad (2\text{-}4)$$

where M is the coefficient of thixotropic breakdown with shear rate. He then used equation (2-4) and (2-3) to derive an equation from the area of thixotropic loop, by which he was able to characterize a thixotropic material with eight constants.

Leonard and Hazlett (19) studied the rheological behavior of aqueous suspensions of Ben-a-gel, a high purified magnesium montmorillonite, by the hysteresis loop method of Green and Weltmann, They found that the plastic viscosities, U, of these suspensions as defined in equation (2-1), could be related to concentration by Arrhenius law at low concentration or Green and Weltmann's equation at higher concentrations. The transition occurs at the concentration at which the gel strength is sufficiently developed so that the suspension no longer flows from an inverted container. At low concentrations, the equation is

$$U=\mu_o e^{kC} \qquad (2-5)$$

and at high concentrations, the equations becomes

$$U=(\mu_o+A)e^{BC} \qquad (2-6)$$

where μ_o is the viscosity of the suspending liquid, C is the concentration and k,A,B are constants.

The concentration of the solute of a solution (or suspension) system is another independent variable in

addition to the previously discussed, shear rate and time, in the study of thixotropic materials.

Modeling Approach

The first model was proposed by Goodeve and Whitfield (20,21) in 1938, they considered that thixotropic system consisted of "cells" or "links", and the concentration of internal structure (cells or links) was the measure of viscosity, or

$$\mu - \mu_o = k'x \qquad (2\text{-}7)$$

where x is the concentration of cells or internal structure, k' is a constant, μ_o is the apparant viscosity at equilibrium. Then they assumed that, under a shear stress, the rate of structural increase of buildup rate will depend on the concentration of "unlinked links" $(x_m - x)$, x_m is the maximum possible concentration of x, i.e.,

$$\frac{dx}{dt} = k''(x_m - x)^a \qquad (2\text{-}8)$$

where a is the order of the reaction and k" is a constant. Their next assumption is that the rate of structural breakdown is proportional to shear rate and structural concentration,

$$\frac{dx}{dt} = k'''x\dot{r} \qquad (2\text{-}9)$$

where k''' is the constant of proportionality.

Equating equation (2-8) and (2-9) under condition of steady state gives

$$x=\frac{k''(x_m-x)^a}{k'''\dot{r}}=\frac{k''x_m^a}{k'''\dot{r}} \qquad (2\text{-}10)$$

Substituting equation (2-10) into (2-7) and making a little arrangement, equation (2-7) becomes

$$K\tau=\mu_o\dot{r}+\theta \qquad (2\text{-}11)$$

where $\theta=\frac{k'k''x_m^a}{k'''}$ is called the "coefficient of thixotropy", μ_o is the viscosity at equilibrium or called residual viscosity, K is a constant. From this approach, equation (2-11) turns out to be the rheological equation of a Bingham plastic material.

Moore (22) made a similar approach as Goodeve did, he assumed a model of dynamic equilibrium between two processes, the natural tendency to buildup the structure and the destruction process due to shear. He assumed the structure parameter x changes according to the equation

$$\frac{dx}{dt}=a(1-x)-bx\dot{r} \qquad (2\text{-}12)$$

where a,b are constants. Integrating equation (2-12) for $\dot{r}$= constant gives

$$x=x_d-(x_d-x_o)e^{-(a+b\dot{r})t} \qquad (2\text{-}13)$$

where $x_d=\frac{a}{a+b\dot{r}}$, and x_o is the value of x at t=0. Assuming the apparent viscosity is linear with x, he finally obtained a rheological equation as

$$\mu_a=\mu_o+cx \qquad (2\text{-}14)$$

where μ_o is the viscosity of the complete structure breakdown and c is a constant. The main difficulty with this model is its inability to explain the yield value.

Eyring and coworkers (23-29) generalized his original absolute reaction kinetics model to thixotropy. They considered the viscosity as a case of absolute reaction rate, through the place exchange mechanism, the unit of flow moving via an energy barrier from one equilibrium position to the nearest in the direction of flow. Therefore they assumed the thixotropic system with two kinds of molecules, entangled and disentangled. Entangled molecules make a three-dimensional nework, in which disentangled and solvent molecules are enclosed. Since the thixotropic flow system consists of both Newtonian and non-Newtonian units, the rheological equation is represented by

$$\tau=\frac{\chi_1\beta_1}{\alpha_1}\dot{r}+\frac{\chi_2}{\alpha_2}\sinh^{-1}\beta_2\dot{r} \qquad (2\text{-}15)$$

where χ_i is the fraction area occupied by the ith kind of flow units; $\frac{1}{\alpha_1}$ and $\frac{1}{\beta_1}$ are the intrinsic shear stress and the intrinsic shear rate for the Newtonian unit, respectively, and $\frac{1}{\alpha_2}$, $\frac{1}{\beta_2}$ are the corresponding quantities for the non-Newtonian units.

Considering the relative amount of entangled and disentangled molecules are determined by the equilibrium constant which is shifted by high shear stress. The net rate of the transition, entangled $\rightleftharpoons$ disentangled is given by

$$\frac{-d\chi_2}{dt} = \chi_2 k_f e^{\lambda c \dot{r}^2/kT} - \chi_1 k_b e^{-(1-\lambda)c\dot{r}^2/kT} \qquad (2\text{-}16)$$

where k_f, k_b is the specific rate for forward reaction and backward reaction at zero shear stress respectively, c is a constant, and λ is a reaction constant.

With the assumption that the backward reaction is very slow at high shear rates with $\dot{r}=\int t$, where $\int$ is a constant determined by experimental condition. Eyring, et al obtained the equation for the upward curve as shown in Figure 1-1. This equation is

$$\tau = \left[1-(\chi_2)_o e^{-k_f \int I}\right]\frac{\beta_1}{\alpha_1}\dot{r} + \frac{1}{\alpha_2}(\chi_2)_o e^{-k_f \int I} \sinh^{-1}\beta_2\dot{r} \qquad (2\text{-}17)$$

The equation for the downward curve is

$$\tau = \left[1-(\chi_2)_0 e^{-k_f \varsigma I_m}\right]\frac{\beta_1}{\alpha_1}\dot{r} + \frac{1}{\alpha_2}(\chi_2)_0 e^{-k_f \varsigma I_m} \cdot \sinh^{-1}\beta_2 \dot{r} \qquad (2\text{-}18)$$

where:

$$\varsigma = (kT/\mu c f^2)^{\frac{1}{2}}$$

$$I = \int_0^{t/\varsigma} e^{t^2/\varsigma^2}\, d(t/\varsigma)$$

Im=value of I at the apex

Brodkey and Denny (30) presented the rheological properties of thixotropy still based on kinetics and upon the assumption that nonlinear characteristics are caused by the structural change. They imagined a reversible reaction between broken and unbroken molecules

$$\text{unbroken} \underset{k_1}{\overset{k_2}{\rightleftharpoons}} \text{broken}$$

The kinetic equation for such a reaction is

$$\frac{-d[\text{unbroken}]}{dt} = k_1'[\text{unbroken}]^n - k_2[\text{broken}]^m \qquad (2\text{-}20)$$

Using the fraction of the quantity, we have

$$\frac{-d\left(\frac{\mu_\theta-\mu_\infty}{\mu_0-\mu_\infty}\right)}{dt} = k_1'\left(\frac{\mu_\theta-\mu_\infty}{\mu_0-\mu_\infty}\right)^n - k_2\left(\frac{\mu_0-\mu_\theta}{\mu_0-\mu_\infty}\right)^m \qquad (2\text{-}21)$$

where μ_0, μ_∞ and μ_θ are the viscosity measured at zero shear rate, high shear rate and any rate of shear respectively, m,n are empirical constants which are related to the order or molecularity of the reaction,

Assuming the order of reaction m=2, n=1 and forward reaction rate constant $k_1'=k_1\dot{r}^p$, where p is interpreted as the susceptibility of the system to shear, they obtained a rheological equation of state in case of $\dot{r}$=constant.

$$\left[2/(b^2-4ac)^{\frac{1}{2}}\right]\cdot\left[\tanh^{-1}(2c\mu_o+b)/(b^2-4ac)^{\frac{1}{2}}\right.$$

$$\left.-\tanh^{-1}\ (2c\mu_\theta+b)/(b^2-4ac)^{\frac{1}{2}}\right]=k_2 t \qquad (2\text{-}22)$$

where:

$$a=(k_1/k_2)\dot{r}^p\mu_\infty+\left[\mu_o^2/(\mu_o-\mu_\infty)\right],$$

$$b=-\left\{(k_1/k_2)\dot{r}^p+\left[2\mu_o/(\mu_o-\mu_\infty)\right]\right\},$$

$$c=1/(\mu_o-\mu_\infty) \qquad (2\text{-}23)$$

One of the main drawbacks to this result is that back calculation to reconstruct the basic shear diagram from the known values of the constants would require more information than the values of the constants and also this equation can not be used to predict the flow curve on the hysteresis loop.

Functional Analysis Approach

This approach of studying thixotropy has appeared in journals in the last few years, Instead of proposing a rheological equation of state for thixotropic fluids, the investigators studied the apparent viscosity and the stress tensor as a functional form which was subjected

to certain restrictions.

Cheng and Evans (31,32) proposed the rheological equation of state for thixotropic fluids as

$$\tau = \mu(x,\dot{r})\dot{r} \tag{2-24}$$

where x is a structural parameter. They expressed the rate equation for structural breakdown as

$$\frac{dx}{dt} = g_{\dot{r}}(x,\dot{r}) \tag{2-25}$$

In order that these equations will describe the rheological behavior of a thixotropic fluid, they postulated the functional forms of τ and $g_{\dot{r}}$ are subjected to certain restrictions as follows

$$\begin{aligned}
&\mu(x,\dot{r}) > 0 \\
&(\partial\tau/\partial\dot{r})_x > 0 \\
&(\partial\tau/\partial x)_{\dot{r}} > 0 \\
&g_{\dot{r}}(x,\dot{r}) = 0 \qquad \text{when } x = x_e(\dot{r}) \\
&g_{\dot{r}}(x,\dot{r}_e) < 0 \qquad \text{when } x > x_e(\dot{r}) \\
&g_{\dot{r}}(x,\dot{r}_e) > 0 \qquad \text{when } x < x_e(\dot{r})
\end{aligned} \tag{2-26}$$

and

$$(\partial g_{\dot{r}}/\partial\dot{r})_x < 0$$

where the subscript e refers to the equilibrium conditions.

The results as we see here, they did do an excellent functional analysis work in the rheological equation for thixotropic fluids, but did not come up with an equation to describe the rheological behavior subject to all of the restrictions.

Harris (33) formulated the rheological equation of state for a time-dependent fluid from the general form of the stress tensor equation

$$\tau_{ij}=2\mu(II,III,t)\dot{r}_{ij} \tag{2-27}$$

where II and III are invariants defined as

$$II=\dot{r}_{ij}\dot{r}_{ji} \tag{2-28}$$

$$III=\dot{r}_{ij}\dot{r}_{jk}\dot{r}_{ki} \tag{2-29}$$

Guided by the fact that there is an undisturbed viscosity which may be recovered following an indefinitely long rest period, he defined a current viscosity deficit by

$$\theta=\mu_1-\mu(t) \tag{2-30}$$

where μ_1 is the undisturbed viscosity and $\mu(t)$ is the viscosity at current time, t, depending on the past flow history.

He assumed that the form of integral equation for the viscosity deficit is

$$\Theta = \int_{-\infty}^{t} f(II,III)M(t-t')dt' \qquad (2-31)$$

where f(II,III) is polynomial in II and III and M(t-t') is an influence function reflecting the effect of the past flow history in the form

$$M(t-t') = \int_{o}^{\infty} (R(t")/t")e^{-(t-t')/t"} dt" \qquad (2-32)$$

where R(t") is a viscosity relaxation spectrum function and t" is the relaxation time. If the oscilatory motion is introduced to the fluid, a first order approximation of viscosity relaxation spectrum function can be obtained, therefore he believed that the rheological equation can be obtained from the data of relaxation spectrum.

Fredrickson (34) recently has suggested that the the constitutive equation of thixotropic material will be Newton's law of viscosity, but with a time-dependent viscosity. He expressed the constitutive equation of thixotropy as

$$\tau(P,t) = \frac{2}{\varphi(P,t)} \dot{r}(P,t) \qquad (2-33)$$

where (P,t) indicates that the rheological quantity is evaluated at material point P at time t, and φ is fluidity, the reciprocal of viscosity.

He then assumed that the rate of change of fluidity at a material point depends on the fluidity and the rate

of strain at that point. Hence the general form of change of fluidity with time is

$$\frac{D}{Dt}\varphi(P,t)=f\left[\varphi(P,t),\dot{r}(P,t)\right] \qquad (2\text{-}34)$$

where D/Dt is material or hydrodynamic derivative. The next assumption in his model is that the function f represents a balance between two processes. The first process is a spontaneous buildup of viscosity (or breakdown of fluidity) which occurs whenever the fluidity becomes greater than its minimum possible value φ_0. The second process is a breakdown of viscosity that occurs whenever shear work is done on the material and its fluidity is less than its maximum possible value φ_∞. Therefore the equation (2-34) can be described as

$$\frac{D\varphi}{Dt}=-g(\varphi-\varphi_0)+h(\varphi_\infty-\varphi,\frac{2}{\varphi}\dot{r}:\dot{r}) \qquad (2\text{-}35)$$

where g and h are non-negative functions such that

$$g(0)=0 \qquad (2\text{-}36)$$

$$h(0,\frac{2}{\varphi}\dot{r}:\dot{r})=h(\varphi_\infty-\varphi,0)=0 \qquad (2\text{-}37)$$

The author finally stated that if g and h are determined by appropriate experiment, the rheological equation of thixotropic fluid can be obtained.

Material Background

Human blood was the material we chose to study its rheological properties. From the viewpoint of rheology, blood can be considered as a concentrated suspension of particles which are about 95% red cell (erythrocytes) and the rest white cell (lycocytes) and platelets. The suspending medium, plasma, contains 7% by weight of proteins-fibrinogen, globulin, and albumin, and 1% of salts and miscellaneous organic compounds (54,60). The behavior of plasma may be approximately characterized as Newtonian. The non-Newtonian is mainly attributed to the presence of the suspended particle (red cells), although the blood becomes highly non-Newtonian in the presence of abnormal proteins and nucleic acid (55).

Physical Properties of Blood

If a healthy blood is allowed to come into contact with surface outside normal living blood vessels, it solidifies unless an anticoagulant is present. This is due to the polymerization of fibrinogen into fibrin in the plasma. The effect of anticoagulant to the rheological properties of blood was studied by several investigators (55-57) and found out that the adding of whole blood with haparin, sequentrene or oxalate makes no significant difference to its behavior other than producing a simple

diluting effect if the anticoagulant is in aqueous solution. Also, Coply (58) recently found that the viscosity is not effected when heparin, Paul's oxalate mixture, or EDTA are mixed in dry form of fresh, undiluted blood. Chien (59) compared the blood treated with heparin or EDTA and the blood with no anticoagulant: He found no significant change in the viscosity of these blood samples.

For temperature effect of blood viscosity, Rutgers (67) has pointed out that the temperature has very little effect on the relative viscosity of suspensions of rigid particles in simple liquids. Rothlin (68) and Azuma (69) showed that the viscosity of blood rose as the temperature fell, which was explained by a small increase in the volume of the individual cells together with an alteration in shape towards a more spherical and less disc-like form. But according to Bugiarello et al (70), they found that for a wide range of haematocrits, the viscosity of human blood relative to plasma was not significantly different at the temperature ranging from 20 to 40^{o}C. Therefore there is no doubt that temperature can effect the viscosity of human blood but the differences are not large.

"Age" is another important factor to rheological behavior of blood. When blood was taken out from human body with anticoagulant added, it was a homogeneous suspension of red cell among plasma, but after 24 hours,

a milky white particle would be found. This is the separation of protein particles from the plasma (55). Since these separated protein particles give an abnormal behavior in rheological measurement, the results of blood measurement are not reliable after 24 hours.

Flow Curve Characteristics of Blood

The flow curve (shear stress versus shear rate) of blood can be obtained from cone-and-plate or other rotational viscometers (to be discussed in a later chapter). The characteristic curve of blood has been treated as a time-independent fluid by numerous investigators as summarized in Whitemore's book (60). The Casson equation (48) is the widely employed equation to represent the flow curve of blood.

The thixotropic behavior of blood was first observed by Copley with coagula of heparinized blood (62). Later, Copley et al. (63) discovered the time-dependent behavior in blood, anticoagulated with heparin, of healthy human subjects. With the recent advancements in instrumentation, it was possible to obtain and record directly reliable experimental data on a graph paper. Cokelet, et al. showed a torque-decay curve of blood at the shear rate 0.01 sec^{-1} (64) obtained from the GDM viscometer (65). Similar torque-decay curves were observed by King and Copley

(66) in a wide range of shear rates obtained from a Weissenberg Rheogoniometer. Wells, et al. (71) found that the physical bonding between the erythrocytes of rouleaux progressively broke down during shearing. The redistribution of single and aggregated erythrocytes eventually reached a state of dynamic equilibrium at each shear rate. At this state further breakdown of rouleaux would not occur as was demonstrated by the authors.

In this thesis, a hysteresis loop of blood which is the crucial test of thixotropy, will be obtained from a modified Weissenberg Rheogoniometer. Two rheological equations of state based on the reversible degradation kinetics are used to represent quantitatively the thixotropy as shown in both the torque-decay curve and the hysteresis loop of human blood.

MATHEMATICAL MODEL

Introduction

Rather complete reviews of the rheological equations have been given by various investigators. It was shown that most of the investigators arbitrarily defined their parameters and randomly selected their experimental conditions for the characterization of thixotropic behavior. The rheological equation (or equations) obtained can only describe part of the overall thixotropic behavior which was illustrated in Figure 1-2 and 1-3. In this chapter the approach is to set up a mathematical model for the kinetics of the isothermal, reversible structural breakdown which characterizes the thixotropic fluid. The degradation reaction which breaks down the aggregated particles (or molecules) is catalyzed by a shear stress. The aggregation reaction, which counter-balances the degradation reaction, restores the system toward its equilibrium distribution of aggregated particles and non-aggregated particles. Instead of having only two types of particles as the previous models assumed, in our model we assume there are n-types of particles, with n ranging from one to infinity, which represent the non-aggregated particles and the aggregated particles consisting of two, three,$\cdots$ or n non-aggregated particles. It is

convenient to borrow the notation of polymer chemistry (35). In the model, we consider the system as a physically bonded polymer mixture with a distribution of monomers, dimers, ··· n-mers, respectively. The viscosity of the system depends on the distribution of the polymer mixture because a long chain polymer usually has a higher viscosity than a short chain polymer. The distribution function varies with respect to the rate of shear and the duration of the shear stress applied.

Reversible Degradation Model

In our model, it is assumed that a thixotropic fluid consists of a mixture of physically bonded polymers with different numbers of mers. The apparent viscosity of the mixture of polymers is defined by

$$\tau = \mu_a(\dot{r}, t)\dot{r} \qquad (3\text{-}1)$$

where τ is the shear stress; $\dot{r}$, the shear rate and μ_a, the apparent viscosity which is a function of the shear rate and the duration of shear. The apparent viscosity of the polymer mixture is a function of the viscosity and the relative amounts of each polymer and of the monomer. It is assumed that the apparent viscosity can be expressed as a linear combination of individual polymer viscosity with its weight function.

$$\mu_a = \sum_{n=1}^{\infty} G_n(\dot{r}, t)\mu_n \qquad (3\text{-}2)$$

where μ_n is the viscosity of the n-mer and $G_n(\dot{r}, t)$ is the normalized distribution function of the polymer mixture or the molar fraction of n-mer which may be defined as

$$G_n(\dot{r}, t) = \frac{[M_n]}{\sum_{n=1}^{\infty} [M_n]} \qquad (3\text{-}3)$$

where $[M_n]$ is the molar concentration of n-mer in the polymer mixture. Replacing the distribution function in equation (3-2) with concentration form gives the following equation

$$\mu_a = \frac{1}{\sum_{n=1}^{\infty} [M_n]} \sum_{n=1}^{\infty} [M_n]\mu_n \qquad (3\text{-}4)$$

The apparent viscosity of the polymer mixture is then defined as equation (3-4) which is in terms of the concentration of individual polymer and its viscosity. Since the viscosity of n-mer, μ_n, is a function of its molecular weight, It may be assumed to be a simple relationship of the following form,

$$\mu_n = \mu_n(n) = Bn \qquad (3\text{-}5)$$

which most of polymer solution follows. In equation (3-5), B is a constant.

Substituting equation (3-5) into equation(3-4), it gives

$$\mu_a = \frac{B}{\sum_{n=1}^{\infty}[M_n]} \sum_{n=1}^{\infty} n[M_n] \qquad (3\text{-}6)$$

Since $\sum_{n=1}^{\infty} n[M_n]$ represents the total concentration of monomer units in the system, it will be a constant through the process provided that there is no volume change due to the degradation or aggregation reactions. Thus equation (3-6) can be written as

$$\mu_a = \frac{L}{\sum_{n=1}^{\infty}[Mn]} \qquad (3\text{-}7)$$

where $L = B\sum_{n=1}^{\infty} n[M_n]$ is a constant.

In our isothermal reversible degradation model, simultaneous degradation and aggregation reaction take place among polymer system, therefore the molecular weight distribution in the system is continuously changed, until a dynamic equilibrium is reached. The so-called "structural breakdown" or "structural buildup" of the thixotropic material is correspondent to whether the rate of degradation is greater or less than the rate of aggregation. We set up the reversible degradation mechanism as

$$\begin{aligned}
M_n &\underset{k_{a\ 1,n-1}}{\overset{k_{d\ 1,n-1}}{\rightleftharpoons}} M_1 + M_{n-1} \\
M_n &\underset{k_{a\ 2,n-2}}{\overset{k_{d\ 2,n-2}}{\rightleftharpoons}} M_2 + M_{n-2} \qquad (3\text{-}8) \\
&\vdots \\
M_n &\underset{k_{a\ n-1,1}}{\overset{k_{d\ n-1,1}}{\rightleftharpoons}} M_{n-1} + M_1 \\
&(n=2,3,4,\cdots,\ )
\end{aligned}$$

where M_n represents the n-mer; M_1, the monomer; k_d and k_a, the rate constants of degradation and aggregation reactions respectively.

Based on physical and chemical ground, we proposed three assumptions for the reversible degradation reaction.

The first assumption is that the breakdown of a polymer always occurs at the end of the polymer chain. Physically, it means that, among a bundle of entangled linear polymer molecules, the ends of n-mer is the most probable fragment to break away from the n-mer under the shear stress. It can be explained by the probability of shear force shearing due to the entanglement of the polymer molecule with other polymer molecules. Mathematically, it means

$$k_{d\ n-1,1}=k_{d\ 1,n-1} \gg k_{d\ n-2,2} \text{ or } k_{d-n,3} \cdots$$
$$\cdots k_{d\ 3,n-3} \text{ or } k_{d\ 2,n-2}$$

The second assumption is that a polymer build-up occurs only by the reaction of the polymer and a monomer. This can also be explained by the mobility of a polymer. A polymer with smaller molecular weight will have larger mobility. Thus a monomer will have the largest mobility, therefore the largest probability, to find a tip of a polymer to react with. The assumption states

$$k_{a\ n-1,1}=k_{a\ 1,n-1}\gg k_{a\ n-2,2} \text{ or } k_{a\ n-3,3} \cdots$$

$$\cdots k_{a\ 3,n-3} \text{ or } k_{a\ 2,n-2}$$

The third assumption is that all the forward rate constants and the backward rate constants are not a function of chain length. This assumption has been used widely in both free radical and cationic as well as anionic polymerization kinetics. Mathematically, it states

$$k_{d\ 1,1}=k_{d\ 1,2}=k_{d\ 2,1}= \cdots=k_{d\ 1,N}=k_{d\ N,1}=k_d$$

$$k_{a\ 1,1}=k_{a\ 1,2}=k_{a\ 2,1}= \cdots=k_{a\ 1,N}=k_{a\ N,1}=k_a$$

With these assumptions, we may rewrite our reaction scheme as

$$\begin{aligned} M_{n+1} &\underset{k_a}{\overset{k_d}{\rightleftharpoons}} M_n+M_1 \\ M_n &\underset{k_a}{\overset{k_d}{\rightleftharpoons}} M_{n-1}+M_1 \\ &\vdots \\ M_2 &\underset{k_a}{\overset{k_d}{\rightleftharpoons}} 2M_1 \end{aligned} \qquad (3\text{-}9)$$

We shall mention here again that the aggregation rate constant, k_a, is a constant, while degradation rate constant, k_d, is a linear function of shear rate, i.e., the rate of degradation is catalyzed by the shear rate. The kinetic rate equations for the above reactions are

$$\frac{d[M_n]}{dt} = k_d\{[M_{n+1}] - [M_n]\} - k_a[M_1]\{[M_n] - [M_{n+1}]\} \qquad (3\text{-}10)$$

$$\frac{d[M_1]}{dt} = k_d\sum_{n=2}^{\infty}[M_n] + k_d[M_2] - k_a[M_1]\sum_{n=1}^{\infty}[M_n] - k_a[M_1]^2 \qquad (3\text{-}11)$$

here $[M_1]$, $[M_2]$ and $[M_n]$ are the molar concentration of monomer, dimer and n-mer respectively.

Since in the polymer mixture, $[M_2] \ll \sum_{n=2}^{\infty}[M_n]$, equation (3-11) can be simplified to

$$\frac{d[M_1]}{dt} = k_d\sum_{n=2}^{\infty}[M_n] - k_a[M_1]\sum_{n=1}^{\infty}[M_n] - k_a[M_1]^2 \qquad (3\text{-}12)$$

A generating function H(y,t) of chain length distribution is defined as

$$H(y,t) = \sum_{n=2}^{\infty} y^n[M_n] \qquad (3\text{-}13)$$

where y is any real number. Using the technique of z-transformation (36), i.e., multiplying every term of equation (3-10) by y^n and summing up from n=2 to∞, we have

$$\frac{\partial H(y,t)}{\partial t} = k_d\left(\frac{1}{y} - 1\right)H(y,t) - k_a[M_1](1-y)H(y,t) \qquad (3\text{-}14)$$

Letting y=1, equation (3-10) and (3-14) become

$$\frac{dH(1,t)}{dt} = 0 \qquad (3\text{-}15)$$

and

$$\frac{d[M_1]}{dt} = k_dH(1,t) - k_aH(1,t)[M_1] - 2k_a[M_1]^2 \qquad (3\text{-}16)$$

From equation (3-13) and the integration of equation (3-15), it is obvious that

$$H(1,t)=\sum_{n=2}^{\infty}[M_n]=h \tag{3-17}$$

where h is a constant and not a function of time. Substituting equation (3-17) into equation (3-16), we have a nonlinear first order differential equation governing the concentration of monomer with respect to time

$$\frac{d[M_1]}{dt} = k_d h - k_a h[M_1] - 2k_a[M_1]^2 \tag{3-18}$$

When the system of polymer mixture is at equilibrium, the equilibrium rate constant of degradation reaction, k_{de}, from equation (3-18) is

$$k_{de}=k_a\left\{[M_1]_e-(2[M_1]_e^2)/h\right\} \tag{3-19}$$

In order to solve equation (3-16) for the change of $[M_1]$ with respect of time, when the polymer mixture is subjected to a shear rate (or shear stress), it is necessary to know the relationship between the degradation rate constant and the shear rate. It is assumed that there exists a linear relationship between these two

$$k_d=k_{de}(1+f\dot{r}) \tag{3-20}$$

where f is a constant.

Since equation (3-20) indicates that the degradation rate constant is related to how the shear rate was

applied, the rheological equation of the thixotropic fluid depends on the way of shear rate changed. There are two cases we are going to discuss; step change and ramboid change of the shear rate.

Step Change of Shear Rate

In this case, the shear rate is stepped up from one equilibrium point to some other finite point instantaneously and maintained at this value. The degradation rate constant, k_d, is constant through the process. Equation (3-18) is then in the form of generalized Riccati equation (37) with the initial condition of $[M_1]$ at its equilibrium concentration $[M_1]_e$, the solution of equation (3-18) is

$$[M_1] = \frac{A}{4k_a} \frac{\tanh(0.5At)+C}{C\cdot\tanh(0.5At)+1} - 0.25h \qquad (3\text{-}21)$$

where

$$A=\sqrt{(k_a h)^2+8k_a k_d h} \qquad (3\text{-}22)$$

and

$$C=\frac{4k_a [M_1]_e+k_a h}{A} \qquad (3\text{-}23)$$

It is shown in equation (3-21) that the monomer concentration is a monotonic function as we expected. Substituting equations (3-21),(3-20) and (3-7) into equation (3-1), the equation of torque decay curve can be expressed by this equation

$$\tau = \frac{L}{0.75h+\frac{A}{4k_a}\left\{\frac{C+\tanh(0.5At)}{1+C\tanh(0.5At)}\right\}}\dot{r} \quad (3\text{-}24)$$

where A,C and k_d are defined in equations (3-22),(3-23) and (3-20) respectively. As time approaches infinite, the shear stress will reach a constant value. It can be represented by the following form

$$\tau\Big|_{t=\infty} = \frac{L}{0.75+\frac{A}{4k_a}}\dot{r} \quad (3\text{-}25)$$

Ramboid Change of Shear rate

In this case, the shear rate is increased linearly from one equilibrium point to some finite point and then decreased linearly to the original equilibrium point, then we say a "cycle" is completed. The cycle can be expressed mathematically as

$$\dot{r}=mt+p \quad (3\text{-}26)$$

where

$p=0, m=m$ when $0 \leq t \leq t_m$;

$p=2mt_m, m=-m$ when $t_m \leq t \leq 2t_m$

where m is a positive constant representing the rate of change of the shear rate with respect to time; p, a constant; t_m, the time required for the shear rate to reach its maximum value.

Combining equation (3-20) and (3-26), it is apparent that

$$k_d h=k_{de}h(1+fp)+k_{de}hfmt=a+bt \qquad (3\text{-}27)$$

where a and b are constants as defined in equation (3-27).

Substituting equation (3-27) into equation (3-18), the change of monomer concentration under the ramboid change of shear rate becomes

$$\frac{d[M_1]}{dt} =a+bt-k_a h[M_1] -2k_a [M_1]^2 \qquad (3\text{-}28)$$

which is a generalized Riccati equation (36), In order to obtain an analytic solution in a closed form, a series of transformations (39,40) is performed. First, it is assumed that

$$[M_1] =w-0.25h \qquad (3\text{-}29)$$

where w is a function of t as defined by equation (3-29), then equation (3-28) is transformed as

$$\frac{dw}{dt} = a+[(k_a h^2)/8] +bt-2k_a w^2 \qquad (3\text{-}30)$$

For second transformation, we let

$$w=(du/dt)/2k_a u \qquad (3\text{-}31)$$

where u is a function of t, thus equation (3-30) becomes

$$\frac{d^2u}{dt^2} - (\alpha+\beta t)u=0 \qquad (3\text{-}32)$$

where

$$\alpha=2ak_a+(k_a^2\ h^2)/4 \qquad (3\text{-}33)$$

$$\beta=2bk_a \qquad (3\text{-}34)$$

where α and β are positive constants as defined by equations (3-33) and (3-34) respectively. The last transformation is introduced as

$$z=(\alpha+\beta t)/\beta^{2/3} \qquad (3\text{-}35)$$

thus the equation (3-32) yields the following form.

$$\frac{d^2u}{dz^2} - zu=0 \qquad (3\text{-}36)$$

The solution of equation (3-36) is a linear combination of a pair Airy functions which are tabulated in some mathematical handbook (38,37).

$$u=K_1A_i(z)+K_2B_i(z) \qquad (3\text{-}37)$$

where $A_i(z)$ and $B_i(z)$ are linearly independent Airy functions; K_1 and K_2 are integrating constants.

$$A_i(z)=C_1F(z)-C_2G(z) \qquad (3\text{-}38)$$

$$B_i(z)=3^{\frac{1}{2}}(C_1F(z)+C_2G(z)) \qquad (3\text{-}39)$$

with

$$C_1=A_i(0)=0.3550280$$

$$C_2=A_i'(0)=0.25881940$$

$$F(z)=\sum_{k=0}^{\infty} 3^k(1/3)_k \left[z^{3k}/(3k!)\right] \qquad (3\text{-}40)$$

$$G(z)=\sum_{k=0}^{\infty} 3^k(2/3)_k \left[z^{3k+1}/(3k+1)!\right]$$

Inverse transformation of equation (3-37) gives the monomer concentration for a ramboid change of shear rate as

$$\left[M_1\right] = \frac{\beta^{\frac{1}{3}}\left\{\left[dA_i(z)/dz\right]+K\left[dB_i(z)/dz\right]\right\}}{2k_a\left[A_i(z)+KB_i(z)\right]} - 0.25h \qquad (3\text{-}41)$$

where $K=K_2/K_1$, a constant.

Since the system is initially at equilibrium, the constant K can be evaluated at t=0, where $\left[M_1\right]=\left[M_1\right]_e$.

$$K= \frac{A_i'(\alpha)-gA_i(\alpha)}{B_i'(\alpha)+gB_i(\alpha)} \qquad (3\text{-}42)$$

where

$$g=(2k_a/\beta^{1/3})(\left[M_1\right]e +0.25h)$$

and

$$\alpha = \alpha/\beta^{2/3}$$

Knowing $\left[M_1\right]$ from equation (3-41), the rheological equation of state for the hysteresis loop can be obtained from equation (3-7) and (3-1) as

$$\tau = \frac{L}{0.75h+\dfrac{\beta^{1/3}\left[A_i'(z)+KB_i'(z)\right]}{2k_a\left[A_i(z)+KB_i(z)\right]}}\,\dot{r} \qquad (3\text{-}43)$$

where

$$z=(\alpha+\beta t)/\beta^{2/3}$$

It is shown that our approach leads to two equations which can quantitatively describe the rheological characteristics of thixotropic fluids. The torque-decay curve corresponds to equation (3-24) and the hysteresis loop is represented by equation (3-43). In our model, these equations consist of five independent parameters, namely L, h, k_a, f and $[M_1]_e$. Once the experimental data of the torque-decay curve and the hysteresis loop are available, these parameters may be obtained by the technique of non-linear parameter estimation (41). Since each of these five parameters has its own physical meaning in the model, these parameters may be used to characterize thixotropic fluids quantitatively.

EXPERIMENTAL DEVICE AND CALIBRATION

Introduction

Most common experimental devices for viscosity measurement fall into two categories; capillary tube and rotational instruments. The rotational type includes the concentric cylinder and the cone-and-plate viscometer.

The capillary viscometer (43,44) is the simplest device for studying the flow properties of liquids. It contains a fluid reservoir connected with a fine-bored tube. The fluid to be studied is stored in the reservoir and forced through the capillary tube by the action of gas pressure, gravity, or a partial vacuum at the exit. The viscosity of the liquid is determined from the measured volumetric flow rate, applied pressure and tube dimensions. Since the capillary viscometer can neither produce a change of shear rate nor keep an uniformly distributed shear stress in the capillary, the rotational viscometer is designed to meet these requirements.

A concentric cylinder or Couette type viscometer is a widely used rotational viscometer in measuring thixotropic fluids (49,50,52). It consists of a pair of coaxial cylinders so arranged that the outer cylinder can be rotated whereas the inner is kept fixed. The fluid to be tested is

held in the gap between the cylinders. The shear stress is measured by the angular deflection of the inner cylinder-the shear rate is measured by its rotational speed. Since the conventional concentric cylinder viscometer suffers the disadvantages of shear rate variation across the annulus, end effects and operating difficulties, the cone-and-plate viscometer was designed to avoid these troubles.

The cone-and-plate viscometer contains a rotating plate and a fixed cone. The fluid is filled between the cone and the plate. If the angle between the cone and the plate is small, the shear rate in the fluid is very nearly uniform throughout the gap. Measurement of rotational speed and torque required to drive the cone yields the shear rate-shear stress relation of the fluid.

In this experimental measurement, a modified Weissenberg Rheogoniometer, which is a cone-and-plate viscometer, is used to provide experimental data for bloods, we will discuss it later.

Original Weissenberg Rheogoniometer

The Weissenberg Rheogoniometer (Figure 4-1) which is one of the most versatile instruments in rotational viscometry was designed by Weissenberg and is manufactured by Farol Research Engineers Ltd., England.

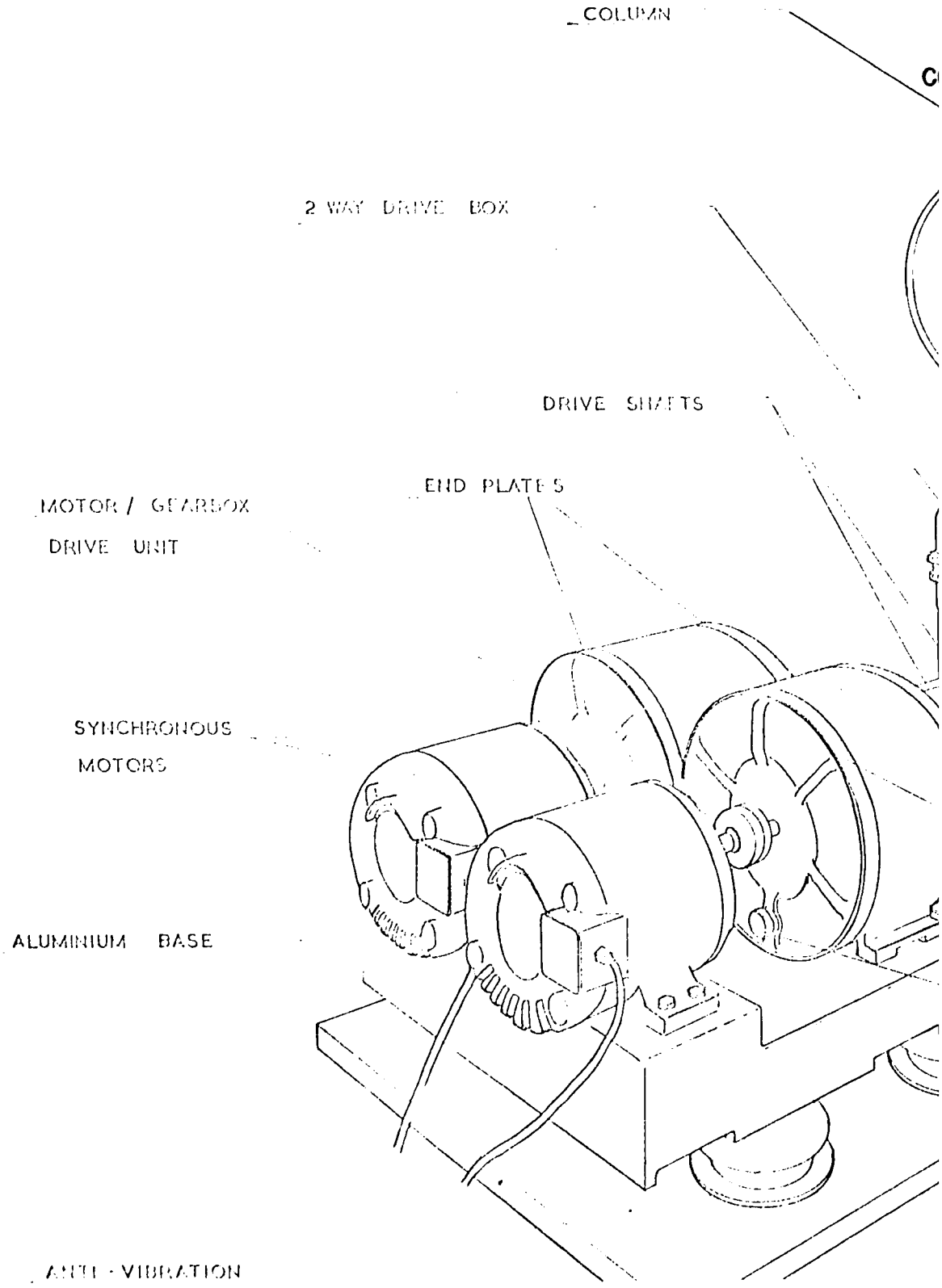
COLUMN
2 WAY DRIVE BOX
DRIVE SHAFTS
END PLATES
MOTOR / GEARBOX
DRIVE UNIT
SYNCHRONOUS
MOTORS
ALUMINIUM BASE
ANTI - VIBRATION

FIGURE 4-1

COMERCIAL RHEOGONIOMETER

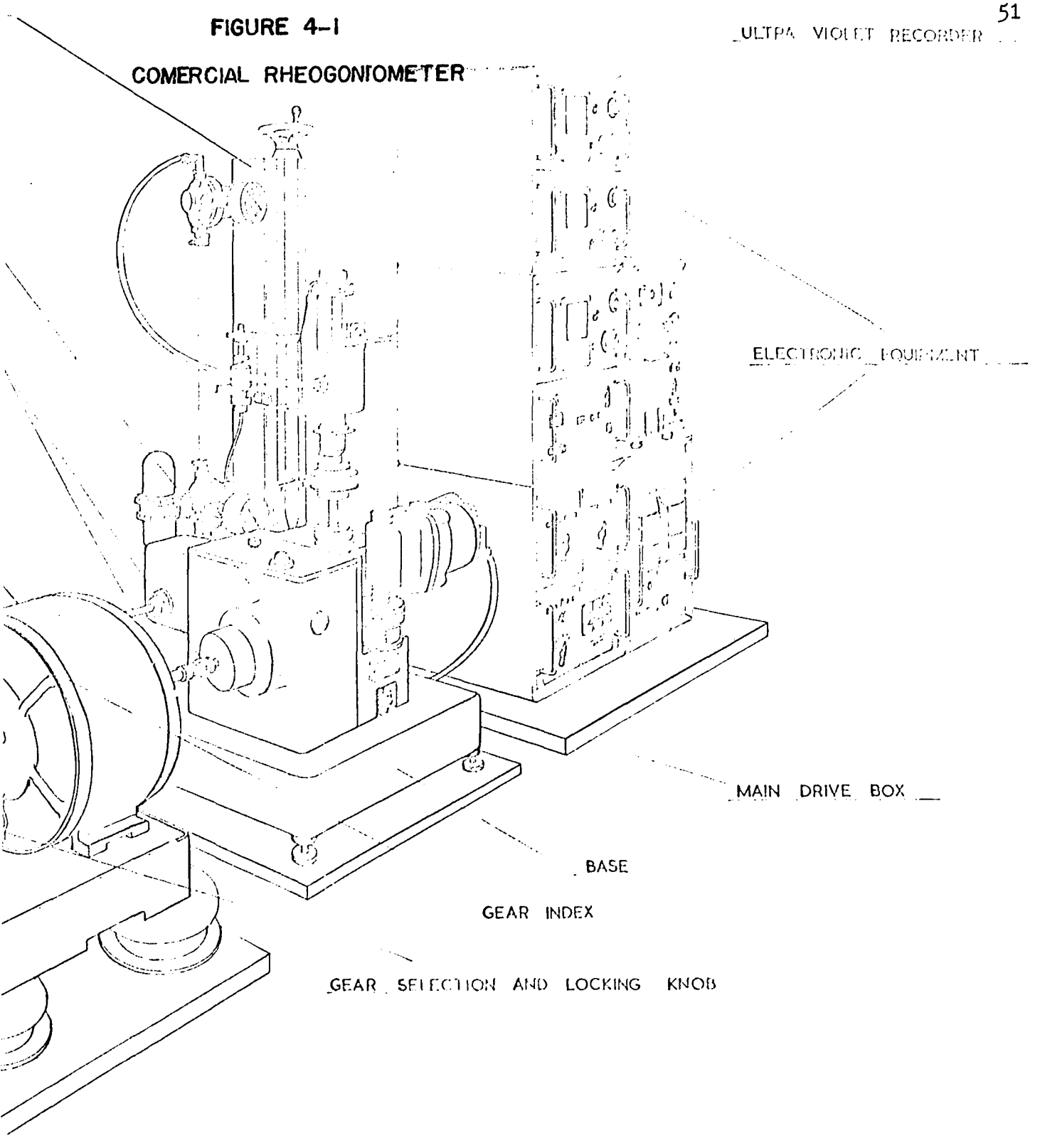

The basis of the device is a simple cone-and-plate viscometer, but it was designed and developed to measure the shear rate-shear stress relation for any kind of fluids in both tangential and normal planes. As the block diagram shows in Figure (4-2), it consists of three major parts; the drive unit, the measuring system, and the control and read-out system.

The drive unit contains a 1 h.p., 1800 RPM synchronous motor which may drive a gear box with gear ratios from 1:1 to $1:10^{5.9}$ in sixty logarithmic steps. The gear box is then coupled to the measuring head with 4 to 1 reduction of RPM via an electromagnetic clutch which can be energized or released at two different current settings. All of the forgoing instruments are located on a bench separated from that for the measuring head.

The head of the measuring system is rigidly constructed and contains the measuring faces (platen-platen, platen-and-cone, or cone-and-cone), a torsion rod, and a constant temperature chamber. The torsion rod is used to detect the movement of upper cone as the measurement of shear stress.

The third part of the instrument consists of various controllers and recorders. The signals from the transducers are picked up by "Penderford Multimeters" whose signals can, in turn, be displayed on an x-y recorder or photographed

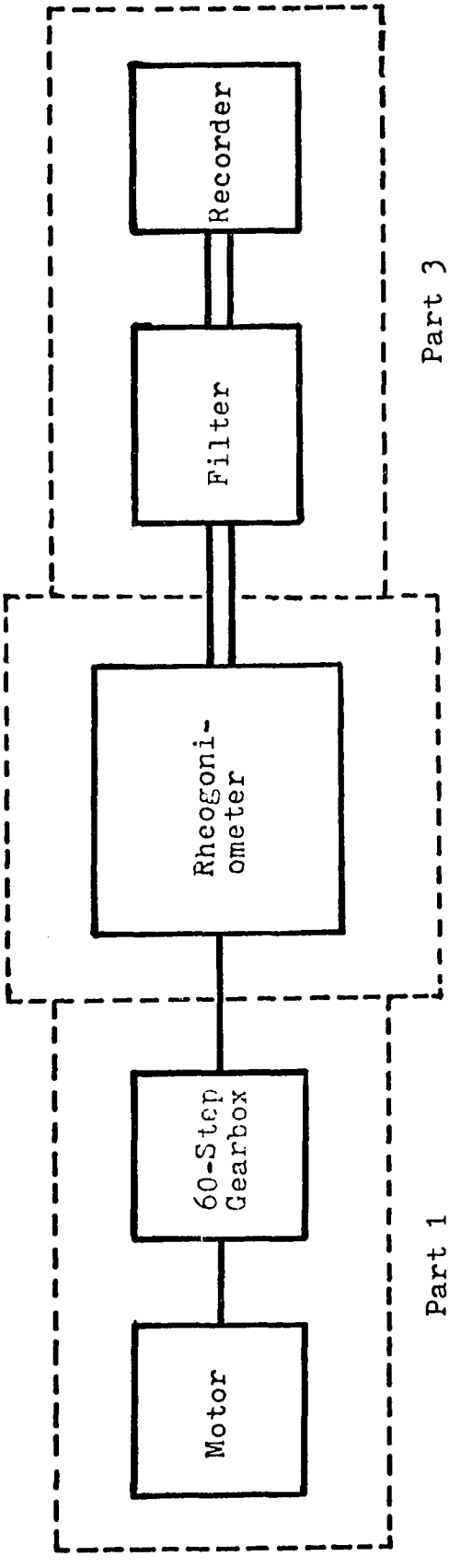

Figure 4-2

Block Diagram of Original
Rheogoniometer

from an oscilloscope screen. The transducer meter is calibrated to read linear displacement directly in microns with ranges of 5 to 2000 microns of full-scale deflection.

The sensitivity of the viscometer is that the viscosity of fluids can be measured from 100 million poise, the thickest bitumens and similar material, down to 0.0001 poise, near the viscosity of air. The range of shear rates available for this viscometer is from 7×10^{-4} sec.$^{-1}$ to 9×10^{3} sec.$^{-1}$, almost covering every possible range. The selection of desired range for particular material can be accomplished by a careful selection of torsion bars, platen diameters, cone angles, and gear box settings.

The plates and cones of the viscometer are available in diameters of 2.5, 5.0, 7.5, 10.0 cm.. The angles of the cone from the horizontal may be $\frac{1}{2}$, 1, 2, or 4^{o}. There are also three interchangeable bars available for choice.

For temperature control, the platens are surrounded by a hinged chamber through which is circulated a heat-exchange fluid. This arrangement is used up to 150^{o}C. For temperature up to 350^{o}C, an electric oven is substituted. A thermocouple is embedded in the surface of each of upper cones so that the temperature of that boundary is known. The detachable cones are insulated such that heat loss into the drive shaft or torsion bar is minimized.

Since the rheogoniometer was designed for a constant shear rate measurement, the results of each measurement becomes point-wise. This means that the Rheogoniometer can only give a step change of shear rate, but not possible for a continuously change of shear rate. Thus, a few modifications were made to the instrument before a set of representative curves can be obtained.

Modified Rheogoniometer

The original Weissenberg Rheogoniometer was modified with a continuously variable speed drive which enabled us to change the angular velocity of the plate linearly from zero to a predetermined maximum value and back to zero. A block diagram of the modification is shown in Figure (4-3). A 1800 RPM synchronous motor was connected to a Graham-200 continuously variable speed drive, fitted with a linear cam which provided a linear change in the angular velocity of the plate. Since the position of linear cam is rotated by a control arm which is driven by a step-function reducer with a constant reversible RPM motor, the input RPM from the synchronous motor is either increased or decreased relying on the direction of movement of the control arm. The output speed of the variable drive varies from 0 to 525 RPM. It is for our convenience that a microswitch system was designed for reversing the control arm automatically after it reached the predetermined position.

Figure 4-3

Block Diagram of Modified Rheogoniometer

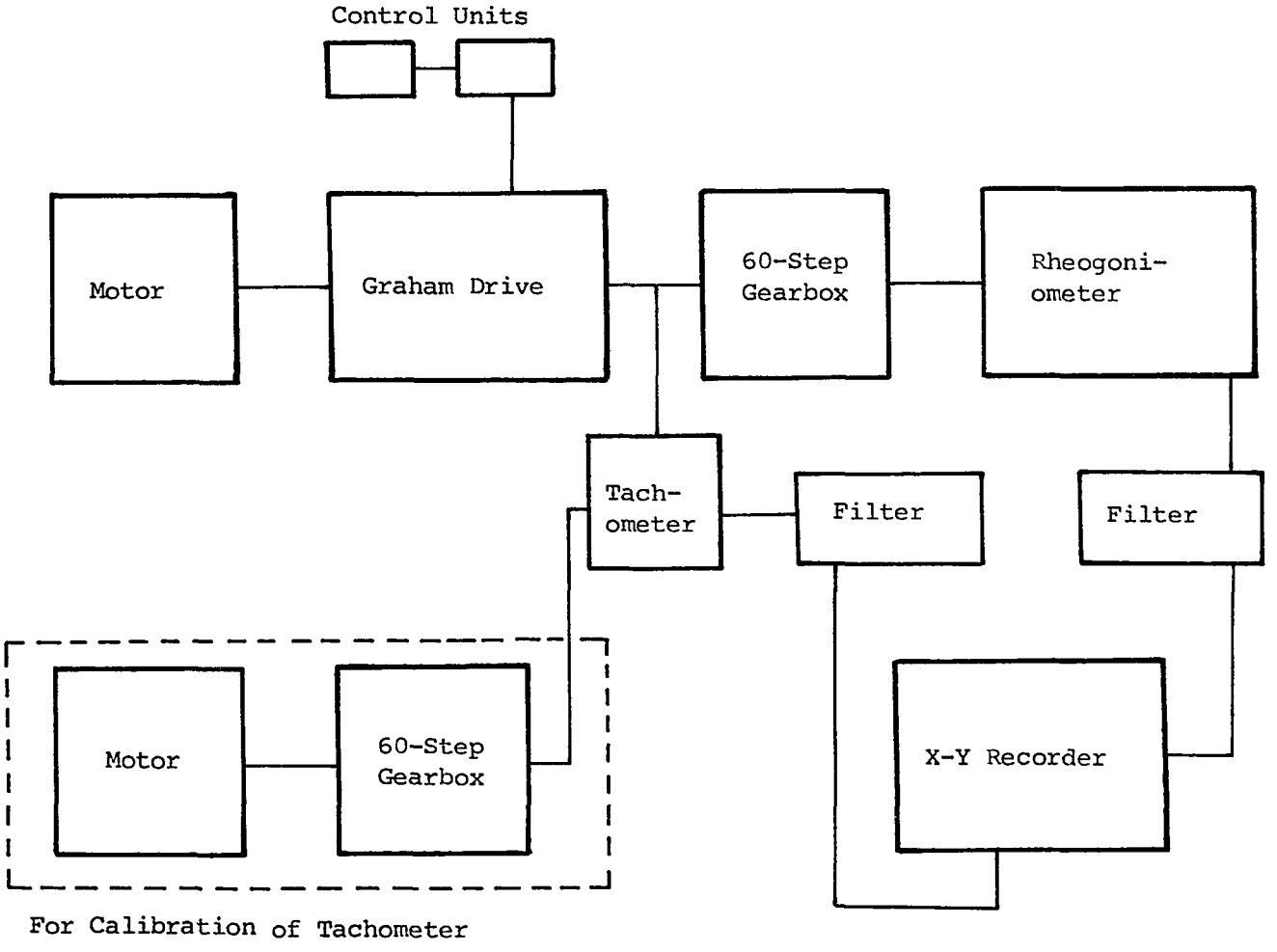

The shear rate measurement in the modified Rheogoniometer was measured by a 45 volt per 1000 RPM Servo-Tek tachometer-generator, connected between the variable drive and 60-step gear box. The voltage which was generated corresponding to the speed of rotation can be detected in the x-y recorder. This allows us to calibrate the relation between RPM of plate and voltage in recorder reading.

Since the original filter is not so perfect to fulfill our requirements, such as response time, cut-off frequency ,···etc., a new designed filter was employed in modified Rheogoniometer (Figure 4-4). The filter was designed to cut the noise from 3 cps to 15 cps and with a 0.15 seconds response time. Moreover, instead of "Penderford Multimeter", a new Omnigraphic 2000 x-y recorder was used to provide a better scale readings.

Working Equation of Rheogoniometer

Since the Rheogoniometer is a simple cone-and-plate viscometer, the torque, T, measured at the top cone of radius, R, (Figure 4-5) is given by

$$T=\int_0^{2\pi}\int_0^R \tau r^2 dr d\phi=(2/3)\pi R^3\tau \qquad (4\text{-}1)$$

or

$$\tau=(3T/2\pi R^3)=(12T/\pi D^3) \qquad (4\text{-}2)$$

where τ is the shear stress in dyne/cm^2. T is torque in

Figure 4-4

Circuit for New Filter

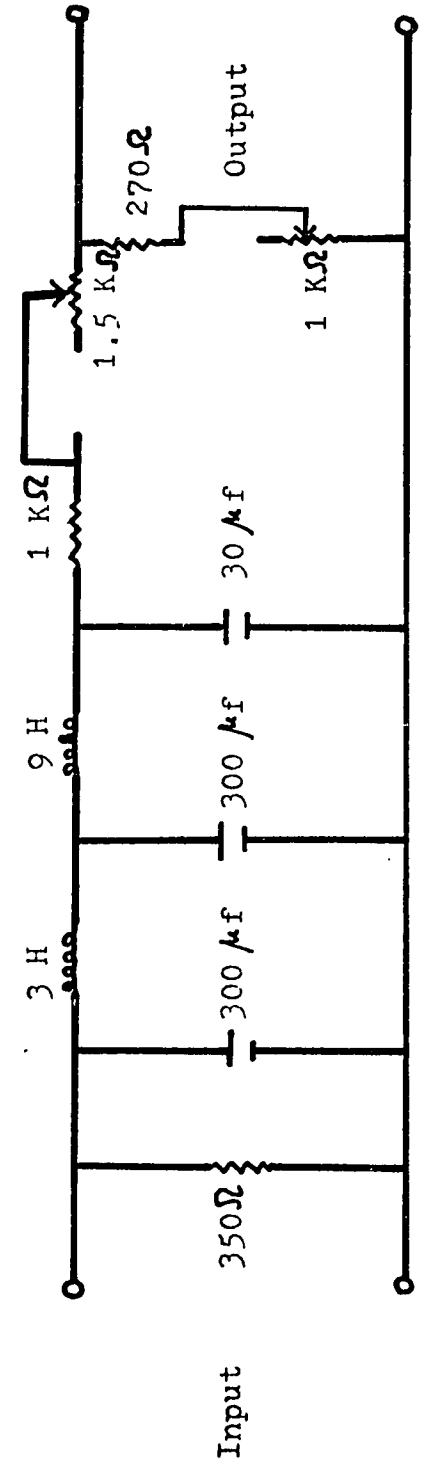

Figure 4-5

Cone-and-plate viscometer

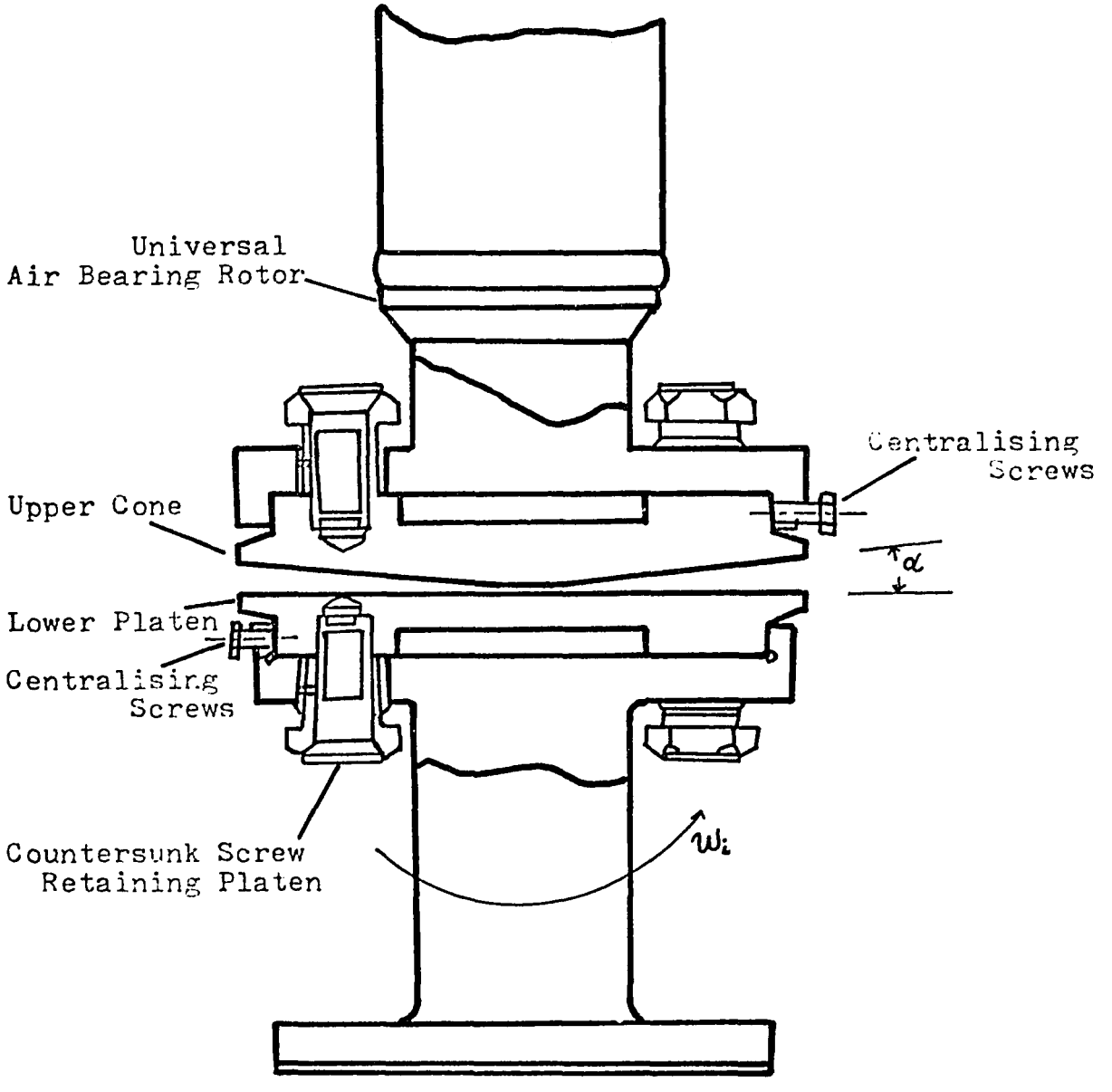

dyne-cm, and D is the diameter of cone and plate in cm.

Since the torque applied to the torsion bar is measured by the movement of the transducer, the torque in equation (4-2) can be re-expressed in terms of transducer displacement.

$$\Delta T = \Delta_T K_T \qquad (4\text{-}3)$$

where K_T is the torsion bar constant in dyne-cm per micron movement of the transducer, and Δ_T is the movement of torsion head transducer in microns.

Substituting equation (4-3) into (4-2), the equation becomes

$$\tau = 12\Delta_T K_T / \pi D^3 \qquad (4\text{-}4)$$

For the actual torque measurement, the voltage rather transducer movement was found in X-Y recorder. Thus, it is necessary to relate the transducer displacement into voltage reading of the recorder. If all the meter settings are kept at the same values, the recorder reading then directly corresponds to the displacement of the transducer, therefore

$$\Delta_T \propto (\text{div}) \qquad (4\text{-}5)$$

and

$$(\Delta_T)_m \propto (\text{div})_m \qquad (4\text{-}6)$$

where (div) is the reading of the shear stress-axis of the recorder in divisions or inches, $(\Delta_T)_m$ is the maximum movement of torsion head transducer in microns, and $(div)_m$ is the maximum recorder reading for full scale deflection of transducer meter in inches.

Dividing equation (4-5) by (4-6), we have

$$(\Delta_T)/(\Delta_T)_m=(div)/(div)_m \qquad (4-7)$$

Combination of equation (4-7) and (4-4), it gives

$$\tau = \left[12(K_T)(\Delta T)_m(div)\right]/\left[\pi D^3(div)_m\right] \qquad (4-8)$$

Equation (4-8) can be used to calculate the shear stress in actual measurements.

As shown in Figure (4-6), the shear rate applied to the lower platen is measured by the rotational speed of platen. The linear velocity at any radius r is ω and the gap width at the radius r is $r\cdot\tan\theta$. The rate of shear at radius r is then given by

$$\dot{r}=\omega r/r\cdot\tan\theta=\omega/\tan\theta$$

Since the small angle of cone and gap width, the rate of shear is assumed constant and independent of radius, i.e.,

$$\dot{r}=\omega/\tan\theta\cong\omega/\theta$$

or

$$\dot{r}=180\omega/\pi\delta=360\Omega/\delta \qquad (4-9)$$

where $\dot{r}$ is the shear rate in sec^{-1}, δ is the angle of the cone in degree, ω is the angular rotation of plate in radius per second, and Ω is the angular rotation in rev. per second. For convenience, the angular rotation speed in equation (4-9) is expressed in terms of RPM.

$$\dot{r}=6(RPM)_{pl}/\delta \qquad (4\text{-}10)$$

Since there is a 4 to 1 internal reduction from horizontal to vertical within instrumental gears, the input rotational speed to the drive box is

$$(RPM)_{pl}=(RPM)_{shaft}/4 \qquad (4\text{-}11)$$

also

$$(RPM)_{shaft}=(RPM)_{tach}/\Lambda \qquad (4\text{-}12)$$

which is due to the 60-step gearbox speed reduction (Appendix A-1). Here Λ is the gearbox ratio of the 60-step gearbox.

Substituting equations (4-11) and (4-12) into equation (4-10), the shear rate becomes

$$\dot{r}=\frac{1.5(RPM)}{\delta\Lambda} \qquad (4\text{-}13)$$

Equations (4-8) and (4-13) are the formulas to calculate the shear stress and shear rate being applied to the material between cone and plate respectively.

Experimental Calibration and Test

Calibration of Tachometer

Since the rotational speed before entering the 60-step gearbox is measured with tachometer, a measurement between the rotational speed of tachometer and its output voltage is used to calibrate its actual RPM. As shown in Figure (4-3), a drive unit of the instrument without continuous variable transmission is directly connected to the 60-step gearbox. A known rotational speed which was generated by the drive was reduced through the gearbox and coupled to tachometer. The output voltage of tachometer was passed through the filter and measured on X-Y recorder.

The results of measurements, as listed in Table (4-1), were plotted on log—log graph paper (Figure 4-6). It shows that the rotational speed of tachometer is linearly related to its output voltage. By using the data of Table 4-1, a linear equation was obtained by simply least square curve fitting. That is

$$(RPM)_{tach}=73.77441(Voltage)_{tach}-0.741214 \quad (4\text{-}14)$$

Substituting equation (4-14) into (4-13), the shear rate can be re-expressed as

$$\dot{r}=1.5\left[73.77441(Voltage)_{tach}-0.741214\right]/\delta\Lambda \quad (4\text{-}15)$$

TABLE 4-1

DATA OF TACHOMETER CALIBRATION

GEARBOX SETTING	R.P.M. (TACHOMETER)	Y-RANGE (volts/in.)	DIVISION (in.)	VOLTS (volts)
0.5	568.0	1.0	7.68	7.68
0.6	452.0	1.0	6.13	6.13
0.7	359.6	1.0	4.89	4.89
0.8	286.0	1.0	3.90	3.90
0.9	227.2	1.0	3.11	3.11
1.0	180.0	1.0	2.48	2.48
1.1	143.2	0.5	3.92	1.96
1.2	113.6	0.5	3.12	1.56
1.3	90.4	0.5	2.50	1.25
1.4	72.0	0.2	4.95	0.99
1.5	56.8	0.2	3.92	0.784
1.6	45.2	0.2	3.13	0.626
1.7	35.96	0.2	2.50	0.500
1.8	28.6	0.1	3.90	0.390
1.9	22.72	0.1	3.11	0.311
2.0	18.0	0.1	2.49	0.249
2.1	14.32	0.1	1.96	0.196
2.2	11.36	0.05	3.14	0.157
2.3	9.04	0.05	2.50	0.125
2.4	7.20	0.02	4.86	0.0972
2.5	5.68	0.02	3.90	0.078
2.6	4.52	0.02	3.10	0.062
2.7	3.596	0.02	2.47	0.0494
3.0	1.80	0.01	2.50	0.025

Figure 4-6

Calibration Curve for
Rotational Speed
of Tachometer

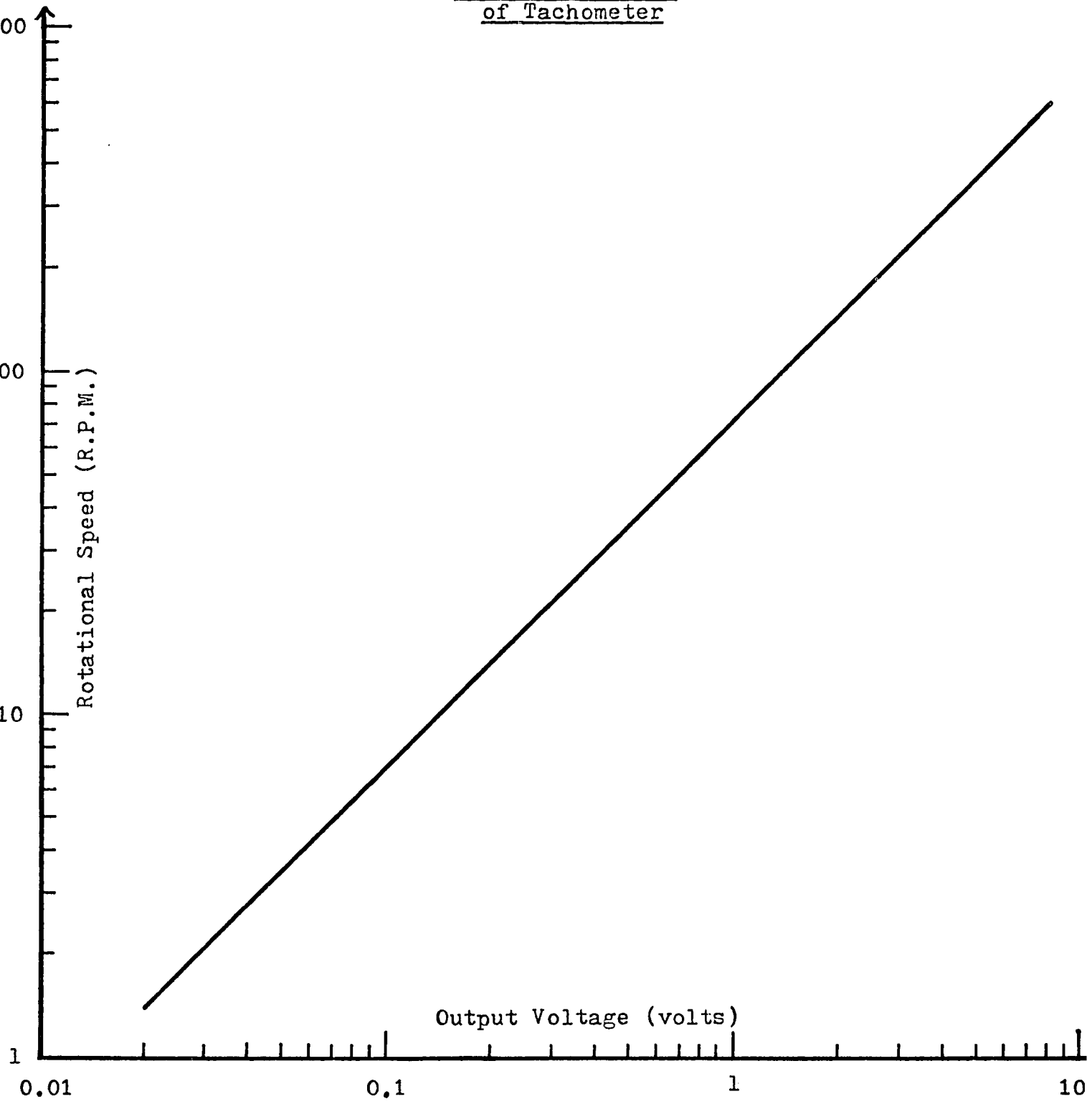

It is more convenient to calculate the shear rate by equation (4-15) than equation (4-13), because of easy measurement of tachometer voltage.

Test of Instrument

Three Standard Brookfield Liquids (Fluid L-5, Fluid L-9 and Fluid L-50) near the viscosity of blood were used to test the reliability of experimental results from the instrument. To ensure this, the reproducibility of flow curve, the accuracy of experimental data, the linearity of shear stress-shear rate relation in ramboid change of shear rate, and the instantaneous stress response in the step change of shear rate were carefully considered.

Since the viscosity of standard liquids is low, a special combination of instrumental accessories is necessary. A 10 cm. plate, 1^{o} cone angle cone, and #7 torsion bar were used in the tests. Furthermore, if the input RPM was too high during the experiment, the material would overcome the surface tension and spread out. This is particularly true for a low viscosity fluid. The shear rate in the experiment was adjusted from 0 to 30 sec^{-1} in ramboid change of shear rate.

The experimental results as shown in Table 4-2 indicates that the average percentage error of the calculated

TABLE 4-2

REPRODUCIBILITY OF INSTRUMENT WITH STANDARD LIQUIDS

STANDARD FLUID	TEMPERATURE (°C)	VISCOSITY (MEASURED) (c.p.)*	VISCOSITY (LISTED) (c.p.)*	PERCENTAGE ERROR (%)
Fluid L-5	25.0	5.16	5.0	3.20
Fluid L-9	25.0	8.75	9.0	2.77
Fluid L-50	25.0	48.70	50.0	2.60

AVERAGE PERCENTAGE ERROR=2.86%

* c.p.=centipoise

viscosity from standard liquids is under 3% when compared to the manufactural specified value. The flow curve (shear stress versus shear rate) on the X-Y recorder is a straight line even after several repeated cycles of ramboid change of shear rate. The response time is 0.15 second for a step change of shear rate. All of these results shows that the instrument is relatively good when we compared with some other commercial apparatus which were found to produce hysteresis loops and have a low response time due to inertia, mechanical and electrical deficiencies in their system.

Experimental Procedure

A set of accessories such as plate diameter, torsion bar, and cone angle were chosen from the instruction manual to give a torque with a desired range, e.g., a measuring of low viscosity material like blood, a big plate, small torsion bar, and little cone angle were chosen to obtain a big signal such that the noise arising from mechanical or electrical vibrations can be overcome. Moreover, the alignment and concentricity of cone and plate were checked; the freedom of movement of torsion bar was tested; the gear box setting was carried out as the value specified on the cone. Then we start the motor.

When the motor was started, the Brake/Drive unit of the electronic control panel was kept in "Brake" position, the

control arm was adjusted to a specified initial rotational speed, the guard ring was around the plate. The sample was taken from constant temperature bath and shaked gently.

Once the sample was placed on the lower plate, the torsion head is screwed down along the column until the upper plate is lowered to the position where the gap setting transducer meter shows zero indication. This means that the distance between cone and plate equals to the required value of gap setting. Liquid will spread over the guard ring out of plate. When this was finished, the Drive/Brake unit was switched to "Drive" position and kept for few seconds until the liquid was sheared enough to reach equilibrium state corresponding to that shear rate, then switched back to "Brake" position. Up to now, we finished the initial step of experiment. The following, we separated into two different experimental procedures for the step and the ramboid change of shear rate.

For the ramboid change of shear rate, after the guard ring (Figure 4-7) was lowered down to renew a fresh surface of the sample (particular surface sensitive materials), the Brake/Drive unit and the microswitch control system were truned to "Drive" and "On" positions simultaneously. Then the control arm would change its position gradually and make the lower plate increase its rotational speed to some predetermined value. When the RPM of the plate reached the

Figure 4-7

Positions of Guard Ring

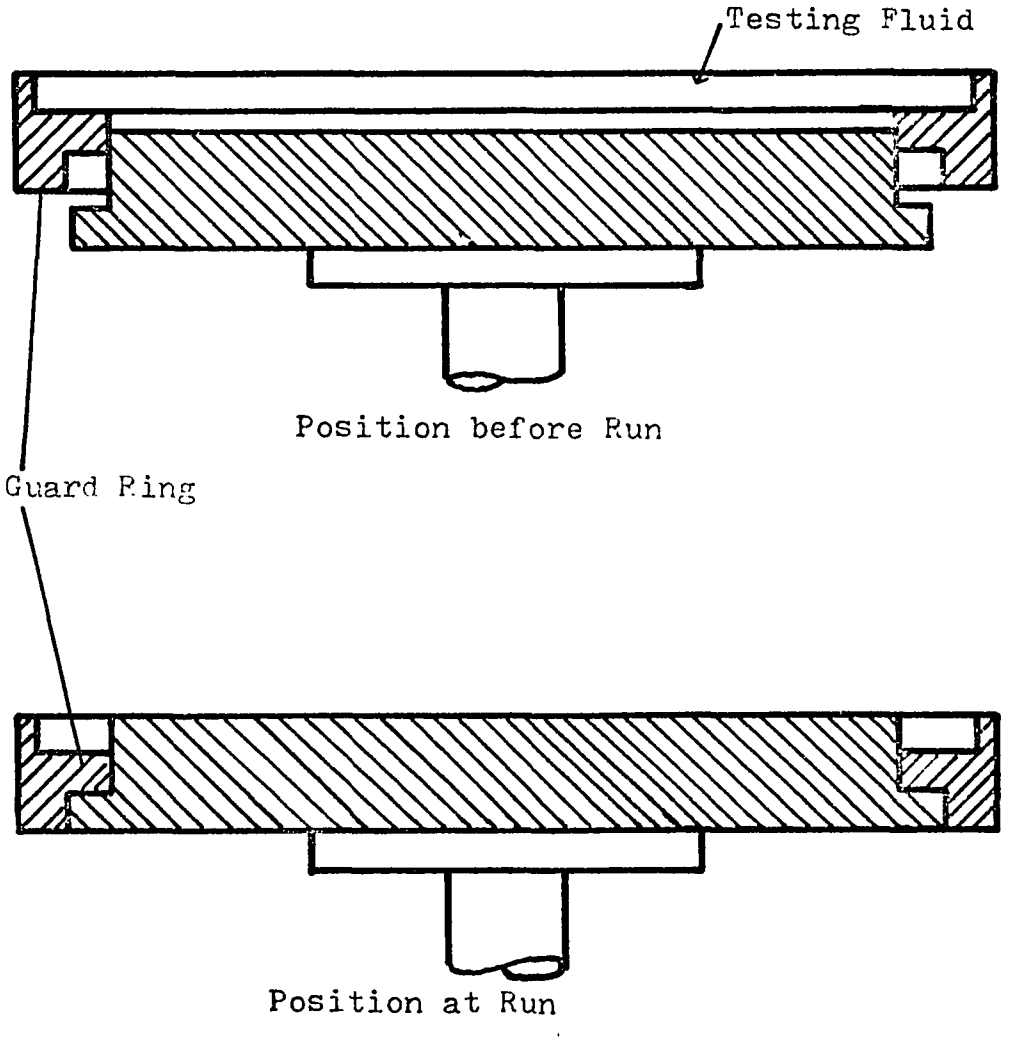

shear rate, the control arm would automatically reverse its direction by microswitch system and decrease RPM linearly to its initial value. The shear stress on the sample would be transmitted from lower plate to upper plate which resulted a movement in the torsion bar transducer and recorded in X-Y recorder.

For the step change of shear rate, the control arm was shifted to a specified position corresponding to a desired shear rate. The guard ring was lowered down and the Brake/ Drive unit was turned to "Drive" position, then the plate jumped up to the particular rotational speed and kept its value. The shear stress was recorded in y axis and time was swept in x direction of X-Y recorder.

When the measurement was finished, the microswitch system was shut down, the Brake/Drive unit was turned to "Brake" position, and the X-Y recorder was set to "Wait" position, then the sample on the plate could be cleaned up If a new measurement was needed, the same procedure as described could be repeated.

RESULTS AND DISCUSSIONS

The experimental results were taken from eight blood samples on the modified Weissenberg Rheogoniometer. Each 100 cc of blood sample contains the following anticoagulants : 0.8 gm of citric acid, 2.2 gm of sodium citrate and 2.45 gm of dextrose. These anticoagulants were used to prevent the blood from clotting. The instrumental arrangements of blood measurements, as listed in Table 5-1, are carefully selected so that the gearbox and the controller can give a shear rate ranging from 0.3325 to 27.9 $sec.^{-1}$ and a cycle time 28.4 sec. in a ramboid change of shear rate, and an instantaneous jump of shear rate to 4.55 $sec.^{-1}$ in a step change of shear rate. The rheogoniometer was fitted with a No. 7 torsion bar and a 10 cm. diameter cone-and-plate with a cone angle of $0^{o}56'53"$. Also the electronic system and the X-Y recorder are well arranged that a maximum sensitivity reading can be obtained.

The room in which the instruments are housed was maintained at temperature $25 \pm 1^{o}C$. It was found that the early norning and the late evening hours were the most suitable times for our experiments because the temperature fluctuation was at its lowest of $25 \pm 0.2^{o}C$.

In order to avoid the denaturing of plasma and surface aging during measurement, a special handling of blood sample

TABLE 5-1

INSTRUMENTAL ARRANGEMENTS AND SETTINGS

INSTRUMENTAL PART	CONTROL VARIABLE	ARRANGEMENT OR SETTING IN RAMBOID CHANGE OF SHEAR RATE	ARRANGEMENT OR SETTING IN STEP CHANGE OF SHEAR RATE
Thermostat	Temperature	25°C	25°C
Gearbox	Gearbox Ratio	1.0	1.0
Rheogoniometer	Plate Diameter	10 cm.	10 cm.
	Cone Angle	56'53"	56'53"
	Gap Setting	41 μ	41 μ
	Torsion Bar No.	#7	#7
Control Unit	Initial Shear Rate	0.332 sec^{-1}	0.332 sec^{-1}
	Rate of Change of Shear Rate	2.0 sec^{-2}	--------
	Cycle Time	28.4 sec.	--------
	Maximum Shear Rate	27.89 sec^{-1}	--------
	Step Change of Shear Rate	--------	4.55 sec^{-1}
Electronic System	Meter Setting	20.0 microns	20.0 microns
	Full Scale Deflection	14.08 in.	14.08 in.
X-Y Recorder	X-range	0.2 volt/in.	1.o sec./in.
	Y-range	0.02 volt/in.	0.01 volt/in.

was performed. After a fresh blood being received from hospital, it was distributed into several small plastic bottles. This gives the protection of blood samples from the air so that the denaturing of plasma might not occur. A constant temperature bath was also employed to maintain the blood at 25°C. Since the blood is a surface sensitive and colloidal fluid, it is very easy to settle during its rheological measurements. A special designed guard ring as illustrated in Figure 4-7 was used to eliminate the possible drying and surface aging.

It is worth mentioning that before the start of blood's measurement, a low shear rate (0.333 $sec.^{-1}$) was applied and maintained in the rheogoniometer until the blood which was held between the cone and the plate reached its equilibrium state corresponding to that shear rate. The reason is that the rheological properties of blood sample depends not only on its shear rate or its shear stress but also on its whole previous rheological history, the necessity to "create" a same starting point before its measurement is quite essential in order to achieve a common reference state for all blood samples.

Results of Measurements in Ramboid Change of Shear Rate

A typical result of blood measurement in ramboid change of shear rate (blood sample B) is given by Figure 5-1 and

Table 5-2. The complete results for all other blood samples are listed in Table A-2 to A-8 (Appendix). These data were obtained from the recorder readings and calculated with equations (4-8) and (4-15), where the torsion bar constant, K_T, is 99.4 dyne-cm/micron, the angle of upper cone is 0.948056°, and the gearbox ratio is 10.0. The reproducibility of shear stress measurements as shown in Table 5-5 was obtained from different blood bottles of the same donor. It is found that the percentage deviation from the chosen bottle is less than 3.5 percent.

As shown in Figure 5-1, a hysteresis loop is found in the flow curve diagram. This phenomenon proves that blood is a thixotropic fluid, because the rheological properties of blood satisfy the accepted definition of thixotropy as quoted earlier in the thesis. The curve also shows that the theoretical predicted values which are calculated from equation (3-43) yield satisfactory representation of experimental data.

The viscosity of blood samples at different shear rate was calculated from equation (1-2) and listed in Table 5-2 and from A-2 to A-8. It was found that the viscosity was decreasing as the blood was subjected to an increase of shear rate and then partially recovered its viscosity when the next half cycle of ramboid change of shear rate began.

TABLE 5-2

COMPARISON OF MODEL PREDICTED VALUES AND EXPERIMENTAL DATA IN RAMBOID CHANGE OF SHEAR RATE

FOR BLOOD B

SHEAR RATE ($sec.^{-1}$)	SHEAR STRESS (MEASURED) ($dyne/cm^2$)		VISCOSITY (MEASURED) (poise)		SHEAR STRESS (PREDICTED) ($dyne/cm^2$)		PERCENTAGE ERROR (%)	
	UPWARD CURVE	DOWNWARD CURVE	UPWARD CURVE	DOWNWARD CURVE	UPWARD CURVE	DOWNWARD CURVE	UPWARD CURVE	DOWNWARD CURVE
2.22	0.620	0.440	0.280	0.198	0.605	0.427	2.48	2.89
3.38	0.781	0.621	0.231	0.183	0.747	0.599	4.36	3.48
4.55	0.901	0.769	0.199	0.166	0.873	0.754	3.14	2.05
5.72	1.02	0.902	0.176	0.156	0.994	0.894	2.75	0.861
6.89	1.12	1.04	0.161	0.149	1.11	1.02	0.965	1.05
8.05	1.20	1.15	0.147	0.141	1.22	1.15	-2.41	1.18
9.22	1.33	1.25	0.143	0.135	1.33	1.26	-0.272	-0.469
11.6	1.53	1.45	0.132	0.125	1.53	1.47	-0.164	-1.29
13.9	1.72	1.66	0.123	0.118	1.72	1.64	-0.076	1.06
16.2	1.89	1.84	0.116	0.112	1.89	1.82	-0.058	1.03
18.6	2.05	2.00	0.111	0.107	2.05	1.98	0.112	0.861
20.9	2.21	2.16	0.106	0.103	2.21	2.16	0.215	0.219
23.2	2.37	2.33	0.102	0.100	2.37	2.30	0.901	1.00
25.6	2.48	2.48	0.0981	0.0981	2.50	2.44	-0.743	1.24
27.9	2.61	2.61	0.0953	0.0953	2.65	2.65	-1.42	-1.42

Figure 5-1

Hysteresis Loop of Blood B in Ramboid Change of Shear Rate

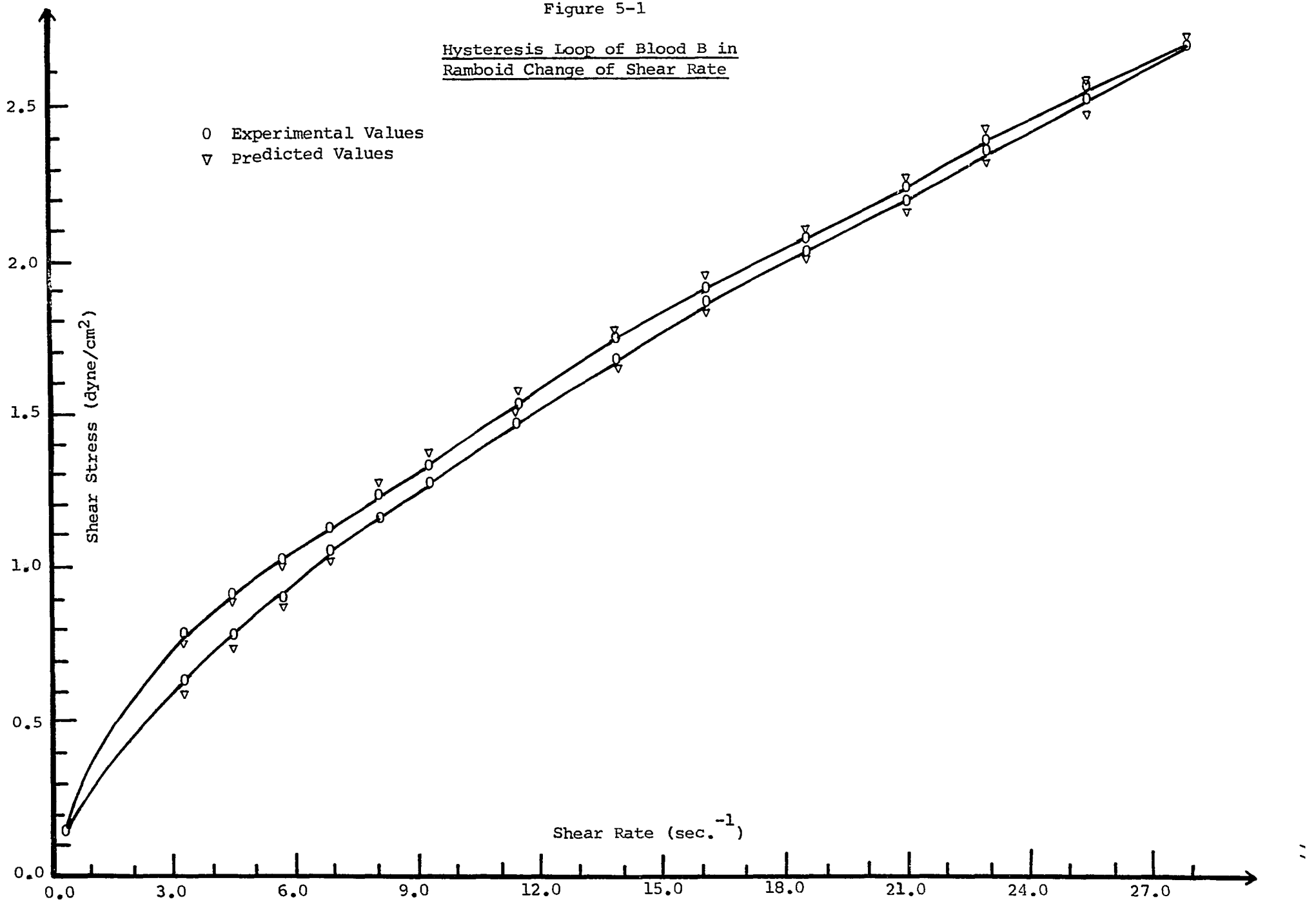

TABLE 5-3

REPRODUCIBILITY OF EXPERIMENTAL SHEAR STRESS IN RABLOID CHANGE OF SHEAR RATE

BLOOD B

BOTTLE No.	TEMPERATURE (^{o}C)	SHEAR STRESS ($dyne/cm^2$)		PERCENTAGE ERROR (w.r.t. BOTTLE 2) (%)	
		UPPER	LOWER	UPPER	LOWER
1	25.0	1.77	1.71	2.91	3.01
2	24.9	1.72	1.66	0.00	0.00
3	25.1	1.66	1.61	-3.49	-3.01

AVERAGE PERCENTAGE ERROR=3.11%

w.r.t.= with respect to

It was also shown that the viscosity of blood samples did not completely restore its initial viscosity as the origin shear rate was returned. It needs a sufficient time for blood samples (about 2 minutes) to have a complete recovery. The comparison of blood viscosity between men (blood samples A-f) and women (blood samples W and Y) was indicated that men's blood is higher viscous than women's. This result becomes more and more important as people try to explain why women have less probability to develop thrombolic disease than men (60,61).

Results of Measurements in Step Change of Shear Rate

The results of blood measurement subjected to a step change of shear rate are given in Table 5-4 and A-9 to A-15. The torque-decay curve of blood B is shown in Figure (5-2). The curve is plotted with shear stress versus time. Since the response time of blood samples (the elapse time between the input and output signal measurement) in a step change of shear rate is quite small (0.15 second) compared to the time to reach its equilibrium shear stress (about 4.0 seconds), the experimental results are considered to be trustworthy.

Comparisons of experimental data and theoretical values are shown in Table 5-4 and A-9 to A-15. It is found that the theoretical representation of torque-decay curves by equation (3-24) are satisfactory. The triangle points in Figure (5-2) represent the predicted values of blood B.

TABLE 5-4

COMPARISON OF MODEL PREDICTED VALUES AND EXPERIMENTAL DATA IN STEP CHANGE OF SHEAR RATE

FOR BLOOD B

TIME (sec.)	SHEAR STRESS (MEASURED) (dyne/cm^2)	VISCOSITY (MEASURED) (poise)	SHEAR STRESS (PREDICTED) (dyne/cm^2)	PERCENTAGE ERROR (%)
0.50	0.939	0.206	0.930	0.960
0.75	0.883	0.194	0.874	1.06
1.00	0.852	0.187	0.840	1.48
1.25	0.830	0.182	0.819	1.34
1.50	0.813	0.179	0.806	0.766
1.75	0.799	0.176	0.799	0.064
2.00	0.786	0.174	0.794	-0.353
2.50	0.783	0.173	0.789	-0.432
3.00	0.782	0.172	0.787	-0.543
3.50	0.780	0.172	0.786	-0.626
4.00	0.780	0.171	0.786	-0.766
4.50	0.780	0.171	0.786	-0.750

Figure 5-2

Torque-decay Curve of Blood B
in Step Change of Shear Rate

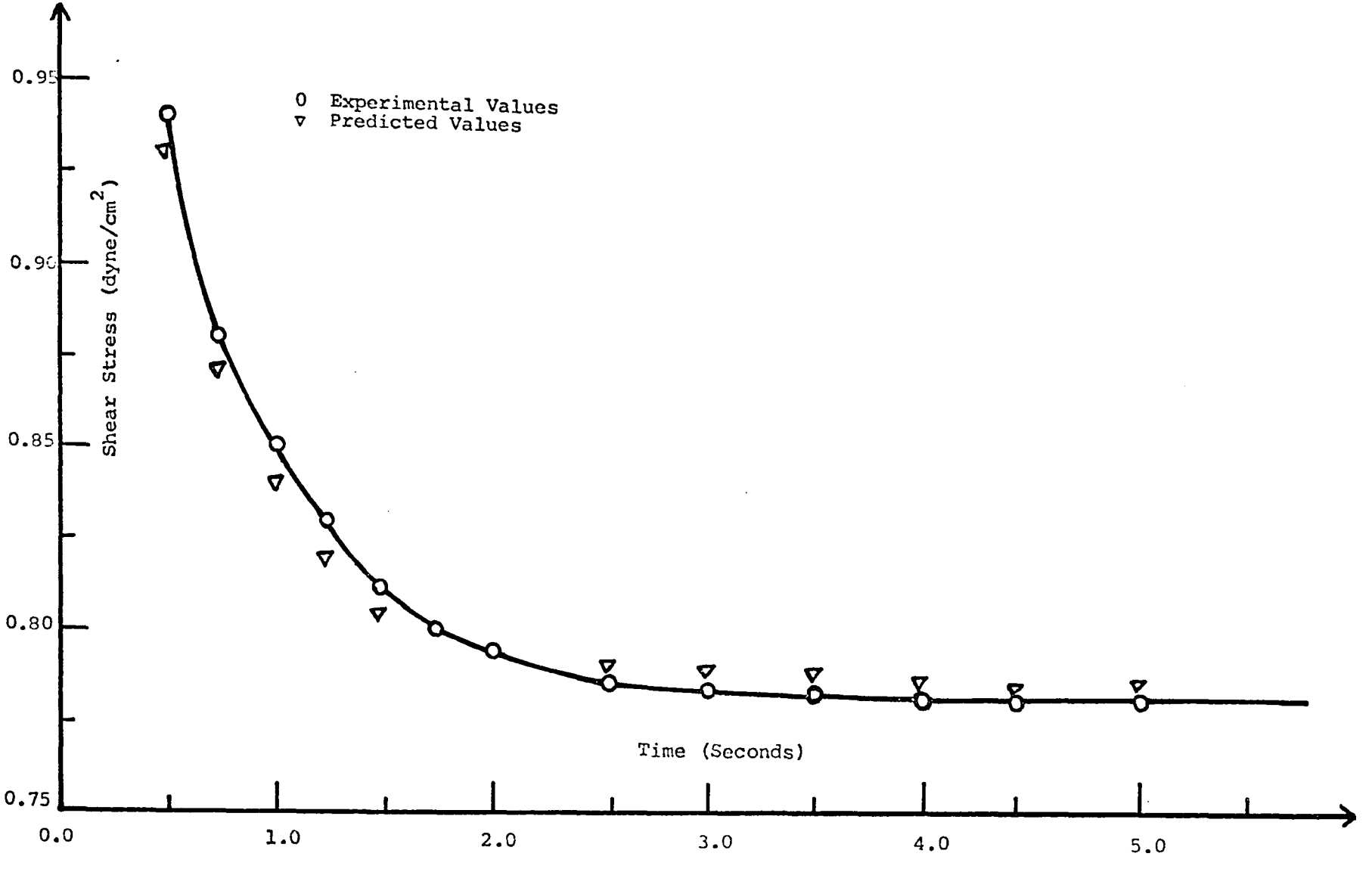

The viscosity of blood samples in a step change of shear rate was obtained from a dividing of torques at different time with its shear rate applied. It was shown that the viscosity decreased sharply in the beginning of its shearing, then slowly reached its equilibrium value and finally became independent of time of shearing.

Estimation of Parameters in Rheological Equations

In order to represent the experimental data with the proposed rheological equations, a FORTRAN program "Least-square Estimation of Nonlinear Parameters" was used to evaluate a set of parameters in the rheological equations. This means equations (3-24) and (3-43) could describe the torque-decay curve and the hysteresis loop with a same set of constants respectively. The program is based on Marquardt algorithm (41) to minimize the least square error between the experimental values and the predicted values from the equations by adjusting the parameters of the equations. That is

$$\Sigma_i (\text{Observed} - \text{Predicted})^2 = \text{Minimum}$$

The program can handle ten independent variables, 500 observable points and 50 adjustable parameters.

Since the proposed rheological equations contain five parameters, $L, h, [M_1]_e, k_a$ and f, a systematic search method is required. The procedure for this estimation is described as follows:

1. Find the rough range of each parameter by increasing (or decreasing) every parameter with some factors such that within these parameter range, the model equation, i.e., equations (3-24) and (3-43), can produce both torque-decay curve and hysteresis loop properly.
2. Minimize the total standard error between the model predicted values and the experimental data (both of torque-decay curve and hysteresis loop) via Marquardt program with two parameters fixed (in this case k_a,f).
3. Repeat procedure (2) until a reasonable limited range of these fixed parameters is obtained.
4. Specify the maximum and minimum possible values of each parameter which was obtained from the precee-ding trials, we finally obtain the parameters of the rheological equations with a minimum standard error.

The results of parameter search for eight blood samples are reported in Table (5-5). It is shown that the standard error of the estimation is about 0.01 dyne/cm^2, within two percent average error with respect to measured shear stress. The relative value of these parameters to eight blood samples was indicated that the blood of high viscosity had greater h and smaller $[M_1]_e$ values than that of low viscosity. This is possibly explained that the blood with higher viscosity contains

TABLE 5-5

MODEL PARAMETERS OF BLOODS

BLOOD	L	h	$[M_1]_e$	k_a	f	STANDARD DEVIATION (dyne/cm^2)
A	0.1494	0.3100	0.2386	0.9901	0.6801	0.01520
B	0.1458	0.3081	0.2452	0.7801	0.6100	0.01740
C	0.1398	0.2759	0.2491	0.8002	0.6002	0.01846
D	0.1176	0.2519	0.2780	0.7100	0.3600	0.009806
E	0.1113	0.2007	0.2842	0.8702	0.4001	0.07817
F	0.1066	0.1750	0.2920	0.8001	0.3303	0.007459
W	0.0906	0.1329	0.3065	0.7600	0.4001	0.01182
Y	0.08415	0.1066	0.3078	0.7502	0.5800	0.009155

more aggregated form of erythrocytes, therefore with bigger value of h; in the other hand, the blood with lower viscosity has less aggregated form of erythrocytes (or more single red cells) with smaller value of $[M_1]_e$.

Since there is no specific information for each donor, we can hardly relate the actual value of k_a and f to the physical-chemical situation of each blood. Theoretically, blood with bigger value of f is easier to degradate an aggregated form to an non-aggregated form of erythrocytes. Therefore it is faster to reach equilibrium state in step change of shear rate or smaller loop in ramboid change of shear rate; less thixotropic. On contrary, a blood with bigger value of k_a is harder to degradate rouleaux into single red cells because of greater counter-degradation rate. Thus, the time to reach equilibrium is longer and the loop is smaller; more thixotropic.

CONCLUSION

The principle accomplishment and contribution of this research can be concluded as follows:

1. The theoretical development of rheological equations based on the model of reversible degradation kinetics can quantitatively describe the rheological behaviors of thixotropic fluids which include the hysteresis loop, the torque-decay curve and various flow curves from the different combinations of these two flow curves. In this model, each of the five parameters in the rheological equations has his own physical meanings which can be used to characterize thixotropic fluids quantitatively. These parameters are: the lump factor of total concentration of non-aggregated units, L; the total aggregated particles concentration, h; the initial equilibrium concentration of non-aggregated particles, $[M_1]_o$; the aggregation rate constant, k_a; and the factor of degradation rate constant induced by shear rate, f.

Since the theoretical equations can quantitatively represent both torque-decay curve and hysteresis loop simultaneously, the rheological equations give a complete representation of the rheological properties of thixotropic fluids. Therefore these equations are considerably better than previously developed equations which either describe only part of rheological behavior or with certain unspecified

functions in the equation.

2. Blood, the most important physiological fluid, was treated as a time-independent fluid (Casson's equation) or a time-dependent fluid (63). This is the first time in the literature that blood shows a hysteresis loop. Therefore it is the first time experimentally proved that blood is a thixotropic fluid.

3. As demonstrated in the Results and Discussion, the derived equations (equations (3-24) and (3-43)) give a excellent representation of rheological data of human blood. This is the first successful trial that the rheological behavior of a thixotropic fluid is quantitatively and completely represented.

4. The modification of the original Weissenberg Rheogoniometer enables the most versatile instrument to generate a hysteresis loop by a linear change of shear rate in the rheological measurement of thixotropic fluids.

5. It has demonstrated from the eight samples of healthy human blood that the rheological properties of blood can be characterized by the five parameters of the derived rheological equations, where parameter h represents the concentration of rouleaux and clumps which are erythrocytes in the aggregated forms; $[M_1]_o$ represents the initial concentration

of the non-aggregated form of erythrocytes; "k_a" is the aggregation rate constant for the individual erythrocytes to form rouleaux or clumps; "f" indicates the rate of degradation of rouleaux into individual erythrocytes catalyzed by the shear; "L" gives the total concentration of individual erythrocytes including both aggregated and non-aggregated form. From Table 5-5, even with limited blood samples studied, it is evident that there are substantial differences in these parameters between males (blood samples A to F) and females (W and Y). The male group shows higher values of L and h, lower values in $[M_1]_o$ than the female group, ie, the male group has higher concentration of total erythrocytes, higher concentration of rouleaux and clumps and lower concentration of individual erythrocytes than the female group. These findings may be used as an explanation why women have less probability to develop thrombolic disease than men. It is believed that the present research may be further developed in future studies as a diagnostic tool for different vascular disorders.

APPENDIX

TABLE A-1

Rotational Speed Reduction of the 60-step Gear Box

GEARBOX SETTING		1500 R.P.M. MOTOR				1800 R.P.M. MOTOR			
		ROTATION		OSCILLATION		ROTATION		OSCILLATION	
RIGHT	LEFT	R.P.M.	SEC/REV.	C.P.S.	SEC/CYCLE	R.P.M.	SEC/REV.	C.P.S.	SEC/CYCLE
0·0	0·0	$3{\cdot}75 \times 10^{-2}$	$2{\cdot}66 \times 10^{1}$	$2{\cdot}50 \times 10$	$4{\cdot}00 \times 10^{-2}$	$4{\cdot}50 \times 10^{-2}$	$2{\cdot}22 \times 10^{1}$	$3{\cdot}00 \times 10$	$3{\cdot}33 \times 10^{-2}$
	0·1	$2{\cdot}98 \times 10^{-2}$	$2{\cdot}01 \times 10^{1}$	$1{\cdot}99 \times 10$	$5{\cdot}03 \times 10^{-2}$	$3{\cdot}58 \times 10^{-2}$	$1{\cdot}68 \times 10^{1}$	$2{\cdot}38 \times 10$	$4{\cdot}20 \times 10^{-2}$
	0·2	$2{\cdot}37 \times 10^{-2}$	$2{\cdot}53 \times 10^{1}$	$1{\cdot}58 \times 10$	$6{\cdot}33 \times 10^{-2}$	$2{\cdot}84 \times 10^{-2}$	$2{\cdot}11 \times 10^{1}$	$1{\cdot}90 \times 10$	$5{\cdot}28 \times 10^{-2}$
	0·3	$1{\cdot}88 \times 10^{-2}$	$3{\cdot}19 \times 10^{1}$	$1{\cdot}26 \times 10$	$7{\cdot}98 \times 10^{-2}$	$2{\cdot}26 \times 10^{-2}$	$2{\cdot}65 \times 10^{1}$	$1{\cdot}51 \times 10$	$6{\cdot}63 \times 10^{-2}$
	0·4	$1{\cdot}50 \times 10^{-2}$	$4{\cdot}01 \times 10^{1}$	$1{\cdot}00 \times 10$	$1{\cdot}00 \times 10^{-1}$	$1{\cdot}80 \times 10^{-2}$	$3{\cdot}34 \times 10^{1}$	$1{\cdot}20 \times 10$	$8{\cdot}35 \times 10^{-2}$
0·5	0·0	$1{\cdot}19 \times 10^{-2}$	$5{\cdot}06 \times 10^{1}$	$7{\cdot}91$	$1{\cdot}27 \times 10^{-1}$	$1{\cdot}42 \times 10^{-2}$	$4{\cdot}22 \times 10^{1}$	$9{\cdot}48$	$1{\cdot}06 \times 10^{-1}$
	0·1	$9{\cdot}43 \times 10$	$6{\cdot}36 \times 10^{1}$	$6{\cdot}28$	$1{\cdot}59 \times 10^{-1}$	$1{\cdot}13 \times 10^{-2}$	$5{\cdot}30 \times 10^{1}$	$7{\cdot}56$	$1{\cdot}33 \times 10^{-1}$
	0·2	$7{\cdot}49 \times 10$	$8{\cdot}01 \times 10^{1}$	$5{\cdot}00$	$2{\cdot}00 \times 10^{-1}$	$8{\cdot}99 \times 10$	$6{\cdot}67 \times 10^{1}$	$6{\cdot}00$	$1{\cdot}67 \times 10^{-1}$
	0·3	$5{\cdot}96 \times 10$	$1{\cdot}01$	$3{\cdot}97$	$2{\cdot}53 \times 10^{-1}$	$7{\cdot}15 \times 10$	$8{\cdot}40 \times 10^{1}$	$4{\cdot}76$	$2{\cdot}10 \times 10^{-1}$
	0·4	$4{\cdot}73 \times 10$	$1{\cdot}27$	$3{\cdot}16$	$3{\cdot}18 \times 10^{-1}$	$5{\cdot}68 \times 10$	$1{\cdot}06$	$3{\cdot}79$	$2{\cdot}65 \times 10^{-1}$
1·0	0·0	$3{\cdot}75 \times 10$	$1{\cdot}00$	$2{\cdot}50$	$4{\cdot}00 \times 10^{-1}$	$4{\cdot}50 \times 10$	$1{\cdot}33$	$3{\cdot}00$	$3{\cdot}33 \times 10^{-1}$
	0·1	$2{\cdot}98 \times 10$	$2{\cdot}01$	$1{\cdot}99$	$5{\cdot}03 \times 10^{-1}$	$3{\cdot}58 \times 10$	$1{\cdot}68$	$2{\cdot}38$	$4{\cdot}20 \times 10^{-1}$
	0·2	$2{\cdot}37 \times 10$	$2{\cdot}53$	$1{\cdot}58$	$6{\cdot}33 \times 10^{-1}$	$2{\cdot}84 \times 10$	$2{\cdot}11$	$1{\cdot}90$	$5{\cdot}28 \times 10^{-1}$
	0·3	$1{\cdot}88 \times 10$	$3{\cdot}19$	$1{\cdot}26$	$7{\cdot}98 \times 10^{-1}$	$2{\cdot}26 \times 10$	$2{\cdot}65$	$1{\cdot}51$	$6{\cdot}63 \times 10^{-1}$
	0·4	$1{\cdot}50 \times 10$	$4{\cdot}01$	$1{\cdot}00$	$1{\cdot}00$	$1{\cdot}80 \times 10$	$3{\cdot}34$	$1{\cdot}20$	$8{\cdot}35 \times 10^{-1}$
1·5	0·0	$1{\cdot}19 \times 10$	$5{\cdot}06$	$7{\cdot}91 \times 10^{-1}$	$1{\cdot}27$	$1{\cdot}42 \times 10$	$4{\cdot}22$	$9{\cdot}48 \times 10^{-1}$	$1{\cdot}06$
	0·1	$9{\cdot}43$	$6{\cdot}36$	$6{\cdot}28 \times 10^{-1}$	$1{\cdot}59$	$1{\cdot}13 \times 10$	$5{\cdot}30$	$7{\cdot}56 \times 10^{-1}$	$1{\cdot}33$
	0·2	$7{\cdot}49$	$8{\cdot}01$	$5{\cdot}00 \times 10^{-1}$	$2{\cdot}00$	$8{\cdot}99$	$6{\cdot}67$	$6{\cdot}00 \times 10^{-1}$	$1{\cdot}67$
	0·3	$5{\cdot}96$	$1{\cdot}01 \times 10$	$3{\cdot}97 \times 10^{-1}$	$2{\cdot}53$	$7{\cdot}15$	$8{\cdot}40$	$4{\cdot}76 \times 10^{-1}$	$2{\cdot}10$
	0·4	$4{\cdot}73$	$1{\cdot}27 \times 10$	$3{\cdot}16 \times 10^{-1}$	$3{\cdot}18$	$5{\cdot}68$	$1{\cdot}06 \times 10$	$3{\cdot}79 \times 10^{-1}$	$2{\cdot}65$
2·0	0·0	$3{\cdot}75$	$2{\cdot}66 \times 10$	$2{\cdot}50 \times 10^{-1}$	$4{\cdot}00$	$4{\cdot}50$	$2{\cdot}22 \times 10$	$3{\cdot}00 \times 10^{-1}$	$3{\cdot}33$
	0·1	$2{\cdot}98$	$2{\cdot}01 \times 10$	$1{\cdot}99 \times 10^{-1}$	$5{\cdot}03$	$3{\cdot}58$	$1{\cdot}68 \times 10$	$2{\cdot}38 \times 10^{-1}$	$4{\cdot}20$
	0·2	$2{\cdot}37$	$2{\cdot}53 \times 10$	$1{\cdot}58 \times 10^{-1}$	$6{\cdot}33$	$2{\cdot}84$	$2{\cdot}11 \times 10$	$1{\cdot}90 \times 10^{-1}$	$5{\cdot}28$
	0·3	$1{\cdot}88$	$3{\cdot}19 \times 10$	$1{\cdot}26 \times 10^{-1}$	$7{\cdot}98$	$2{\cdot}26$	$2{\cdot}65 \times 10$	$1{\cdot}51 \times 10^{-1}$	$6{\cdot}63$
	0·4	$1{\cdot}50$	$4{\cdot}01 \times 10$	$1{\cdot}00 \times 10^{-1}$	$1{\cdot}00 \times 10$	$1{\cdot}80$	$3{\cdot}34 \times 10$	$1{\cdot}20 \times 10^{-1}$	$8{\cdot}35$
2·5	0·0	$1{\cdot}19$	$5{\cdot}06 \times 10$	$7{\cdot}91 \times 10^{-2}$	$1{\cdot}27 \times 10$	$1{\cdot}42$	$4{\cdot}22 \times 10$	$9{\cdot}48 \times 10^{-2}$	$1{\cdot}06 \times 10$
	0·1	$9{\cdot}43 \times 10^{-1}$	$6{\cdot}36 \times 10$	$6{\cdot}28 \times 10^{-2}$	$1{\cdot}59 \times 10$	$1{\cdot}13$	$5{\cdot}30 \times 10$	$7{\cdot}56 \times 10^{-2}$	$1{\cdot}33 \times 10$
	0·2	$7{\cdot}49 \times 10^{-1}$	$8{\cdot}01 \times 10$	$5{\cdot}00 \times 10^{-2}$	$2{\cdot}00 \times 10$	$8{\cdot}99 \times 10^{-1}$	$6{\cdot}67 \times 10$	$6{\cdot}00 \times 10^{-2}$	$1{\cdot}67 \times 10$
	0·3	$5{\cdot}96 \times 10^{-1}$	$1{\cdot}01 \times 10^{2}$	$3{\cdot}97 \times 10^{-2}$	$2{\cdot}53 \times 10$	$7{\cdot}15 \times 10^{-1}$	$8{\cdot}39 \times 10$	$4{\cdot}76 \times 10^{-2}$	$2{\cdot}10 \times 10$
	0·4	$4{\cdot}73 \times 10^{-1}$	$1{\cdot}27 \times 10^{2}$	$3{\cdot}16 \times 10^{-2}$	$3{\cdot}16 \times 10$	$5{\cdot}68 \times 10^{-1}$	$1{\cdot}06 \times 10^{2}$	$3{\cdot}79 \times 10^{-2}$	$2{\cdot}65 \times 10$
3·0	0·0	$3{\cdot}75 \times 10^{-1}$	$1{\cdot}00 \times 10^{2}$	$2{\cdot}50 \times 10^{-2}$	$4{\cdot}00 \times 10$	$4{\cdot}50 \times 10^{-1}$	$1{\cdot}33 \times 10^{2}$	$3{\cdot}00 \times 10^{-2}$	$3{\cdot}33 \times 10$
	0·1	$2{\cdot}98 \times 10^{-1}$	$2{\cdot}01 \times 10^{2}$	$1{\cdot}99 \times 10^{-2}$	$5{\cdot}03 \times 10$	$3{\cdot}58 \times 10^{-1}$	$1{\cdot}68 \times 10^{2}$	$2{\cdot}38 \times 10^{-2}$	$4{\cdot}20 \times 10$
	0·2	$2{\cdot}37 \times 10^{-1}$	$2{\cdot}53 \times 10^{2}$	$1{\cdot}58 \times 10^{-2}$	$6{\cdot}33 \times 10$	$2{\cdot}84 \times 10^{-1}$	$2{\cdot}11 \times 10^{2}$	$1{\cdot}90 \times 10^{-2}$	$5{\cdot}28 \times 10$
	0·3	$1{\cdot}88 \times 10^{-1}$	$3{\cdot}19 \times 10^{2}$	$1{\cdot}26 \times 10^{-2}$	$7{\cdot}98 \times 10$	$2{\cdot}26 \times 10^{-1}$	$2{\cdot}65 \times 10^{2}$	$1{\cdot}51 \times 10^{-2}$	$6{\cdot}63 \times 10$
	0·4	$1{\cdot}50 \times 10^{-1}$	$4{\cdot}01 \times 10^{2}$	$1{\cdot}00 \times 10^{-2}$	$1{\cdot}00 \times 10^{2}$	$1{\cdot}80 \times 10^{-1}$	$3{\cdot}34 \times 10^{2}$	$1{\cdot}20 \times 10^{-2}$	$8{\cdot}35 \times 10$
3·5	0·0	$1{\cdot}19 \times 10^{-1}$	$5{\cdot}06 \times 10^{2}$	$7{\cdot}91 \times 10^{-3}$	$1{\cdot}27 \times 10^{2}$	$1{\cdot}42 \times 10^{-1}$	$4{\cdot}22 \times 10^{2}$	$9{\cdot}48 \times 10^{-3}$	$1{\cdot}06 \times 10^{2}$
	0·1	$9{\cdot}43 \times 10^{-2}$	$6{\cdot}36 \times 10^{2}$	$6{\cdot}28 \times 10^{-3}$	$1{\cdot}59 \times 10^{2}$	$1{\cdot}13 \times 10^{-1}$	$5{\cdot}30 \times 10^{2}$	$7{\cdot}56 \times 10^{-3}$	$1{\cdot}33 \times 10^{2}$
	0·2	$7{\cdot}49 \times 10^{-2}$	$8{\cdot}01 \times 10^{2}$	$5{\cdot}00 \times 10^{-3}$	$2{\cdot}00 \times 10^{2}$	$8{\cdot}99 \times 10^{-2}$	$6{\cdot}67 \times 10^{2}$	$6{\cdot}00 \times 10^{-3}$	$1{\cdot}67 \times 10^{2}$
	0·3	$5{\cdot}96 \times 10^{-2}$	$1{\cdot}01 \times 10^{3}$	$3{\cdot}97 \times 10^{-3}$	$2{\cdot}53 \times 10^{2}$	$7{\cdot}15 \times 10^{-2}$	$8{\cdot}39 \times 10^{2}$	$4{\cdot}76 \times 10^{-3}$	$2{\cdot}10 \times 10^{2}$
	0·4	$4{\cdot}74 \times 10^{-2}$	$1{\cdot}27 \times 10^{3}$	$3{\cdot}16 \times 10^{-3}$	$3{\cdot}18 \times 10^{2}$	$5{\cdot}68 \times 10^{-2}$	$1{\cdot}06 \times 10^{3}$	$3{\cdot}79 \times 10^{-3}$	$2{\cdot}64 \times 10^{2}$
4·0	0·0	$3{\cdot}75 \times 10^{-2}$	$1{\cdot}60 \times 10^{3}$	$2{\cdot}50 \times 10^{-3}$	$4{\cdot}00 \times 10^{2}$	$4{\cdot}50 \times 10^{-2}$	$1{\cdot}33 \times 10^{3}$	$3{\cdot}00 \times 10^{-3}$	$3{\cdot}33 \times 10^{2}$
	0·1	$2{\cdot}98 \times 10^{-2}$	$2{\cdot}01 \times 10^{3}$	$1{\cdot}99 \times 10^{-3}$	$5{\cdot}03 \times 10^{2}$	$3{\cdot}58 \times 10^{-2}$	$1{\cdot}68 \times 10^{3}$	$2{\cdot}38 \times 10^{-3}$	$4{\cdot}19 \times 10^{2}$
	0·2	$2{\cdot}37 \times 10^{-2}$	$2{\cdot}53 \times 10^{3}$	$1{\cdot}58 \times 10^{-3}$	$6{\cdot}33 \times 10^{2}$	$2{\cdot}84 \times 10^{-2}$	$2{\cdot}11 \times 10^{3}$	$1{\cdot}90 \times 10^{-3}$	$5{\cdot}28 \times 10^{2}$
	0·3	$1{\cdot}88 \times 10^{-2}$	$3{\cdot}19 \times 10^{3}$	$1{\cdot}26 \times 10^{-3}$	$7{\cdot}98 \times 10^{2}$	$2{\cdot}26 \times 10^{-2}$	$2{\cdot}65 \times 10^{3}$	$1{\cdot}51 \times 10^{-3}$	$6{\cdot}64 \times 10^{2}$
	0·4	$1{\cdot}50 \times 10^{-2}$	$4{\cdot}01 \times 10^{3}$	$1{\cdot}00 \times 10^{-3}$	$1{\cdot}00 \times 10^{3}$	$1{\cdot}80 \times 10^{-2}$	$3{\cdot}34 \times 10^{3}$	$1{\cdot}20 \times 10^{-3}$	$8{\cdot}35 \times 10^{2}$
4·5	0·0	$1{\cdot}19 \times 10^{-2}$	$5{\cdot}06 \times 10^{3}$	$7{\cdot}91 \times 10^{-4}$	$1{\cdot}27 \times 10^{3}$	$1{\cdot}42 \times 10^{-2}$	$4{\cdot}22 \times 10^{3}$	$9{\cdot}48 \times 10^{-4}$	$1{\cdot}05 \times 10^{3}$
	0·1	$9{\cdot}43 \times 10^{-3}$	$6{\cdot}36 \times 10^{3}$	$6{\cdot}28 \times 10^{-4}$	$1{\cdot}59 \times 10^{3}$	$1{\cdot}13 \times 10^{-2}$	$5{\cdot}30 \times 10^{3}$	$7{\cdot}56 \times 10^{-4}$	$1{\cdot}33 \times 10^{3}$
	0·2	$7{\cdot}49 \times 10^{-3}$	$8{\cdot}01 \times 10^{3}$	$5{\cdot}00 \times 10^{-4}$	$2{\cdot}00 \times 10^{3}$	$8{\cdot}99 \times 10^{-3}$	$6{\cdot}67 \times 10^{3}$	$6{\cdot}00 \times 10^{-4}$	$1{\cdot}67 \times 10^{3}$
	0·3	$5{\cdot}96 \times 10^{-3}$	$1{\cdot}01 \times 10^{4}$	$3{\cdot}97 \times 10^{-4}$	$2{\cdot}52 \times 10^{3}$	$7{\cdot}15 \times 10^{-3}$	$8{\cdot}39 \times 10^{3}$	$4{\cdot}76 \times 10^{-4}$	$2{\cdot}10 \times 10^{3}$
	0·4	$4{\cdot}74 \times 10^{-3}$	$1{\cdot}27 \times 10^{4}$	$3{\cdot}16 \times 10^{-4}$	$3{\cdot}17 \times 10^{3}$	$5{\cdot}68 \times 10^{-3}$	$1{\cdot}06 \times 10^{4}$	$3{\cdot}79 \times 10^{-4}$	$2{\cdot}64 \times 10^{3}$
5·0	0·0	$3{\cdot}75 \times 10^{-3}$	$1{\cdot}60 \times 10^{4}$	$2{\cdot}50 \times 10^{-4}$	$4{\cdot}00 \times 10^{3}$	$4{\cdot}50 \times 10^{-3}$	$1{\cdot}33 \times 10^{4}$	$3{\cdot}00 \times 10^{-4}$	$3{\cdot}33 \times 10^{3}$
	0·1	$2{\cdot}98 \times 10^{-3}$	$2{\cdot}01 \times 10^{4}$	$1{\cdot}99 \times 10^{-4}$	$5{\cdot}03 \times 10^{3}$	$3{\cdot}58 \times 10^{-3}$	$1{\cdot}68 \times 10^{4}$	$2{\cdot}38 \times 10^{-4}$	$4{\cdot}19 \times 10^{3}$
	0·2	$2{\cdot}37 \times 10^{-3}$	$2{\cdot}53 \times 10^{4}$	$1{\cdot}58 \times 10^{-4}$	$6{\cdot}33 \times 10^{3}$	$2{\cdot}84 \times 10^{-3}$	$2{\cdot}11 \times 10^{4}$	$1{\cdot}90 \times 10^{-4}$	$5{\cdot}28 \times 10^{3}$
	0·3	$1{\cdot}88 \times 10^{-3}$	$3{\cdot}19 \times 10^{4}$	$1{\cdot}26 \times 10^{-4}$	$7{\cdot}98 \times 10^{3}$	$2{\cdot}26 \times 10^{-3}$	$2{\cdot}65 \times 10^{4}$	$1{\cdot}51 \times 10^{-4}$	$6{\cdot}64 \times 10^{3}$
	0·4	$1{\cdot}50 \times 10^{-3}$	$4{\cdot}01 \times 10^{4}$	$1{\cdot}00 \times 10^{-4}$	$1{\cdot}00 \times 10^{4}$	$1{\cdot}80 \times 10^{-3}$	$3{\cdot}34 \times 10^{4}$	$1{\cdot}20 \times 10^{-4}$	$8{\cdot}35 \times 10^{3}$
5·5	0·0	$1{\cdot}19 \times 10^{-3}$	$5{\cdot}06 \times 10^{4}$	$7{\cdot}91 \times 10^{-5}$	$1{\cdot}27 \times 10^{4}$	$1{\cdot}42 \times 10^{-3}$	$4{\cdot}22 \times 10^{4}$	$9{\cdot}48 \times 10^{-5}$	$1{\cdot}05 \times 10^{4}$
	0·1	$9{\cdot}43 \times 10^{-4}$	$6{\cdot}36 \times 10^{4}$	$6{\cdot}28 \times 10^{-5}$	$1{\cdot}59 \times 10^{4}$	$1{\cdot}13 \times 10^{-3}$	$5{\cdot}30 \times 10^{4}$	$7{\cdot}56 \times 10^{-5}$	$1{\cdot}33 \times 10^{4}$
	0·2	$7{\cdot}49 \times 10^{-4}$	$8{\cdot}01 \times 10^{4}$	$5{\cdot}00 \times 10^{-5}$	$2{\cdot}00 \times 10^{4}$	$8{\cdot}99 \times 10^{-4}$	$6{\cdot}67 \times 10^{4}$	$6{\cdot}00 \times 10^{-5}$	$1{\cdot}67 \times 10^{4}$
	0·3	$5{\cdot}96 \times 10^{-4}$	$1{\cdot}01 \times 10^{5}$	$3{\cdot}97 \times 10^{-5}$	$2{\cdot}52 \times 10^{4}$	$7{\cdot}14 \times 10^{-4}$	$8{\cdot}39 \times 10^{4}$	$4{\cdot}76 \times 10^{-5}$	$2{\cdot}10 \times 10^{4}$
	0·4	$4{\cdot}74 \times 10^{-4}$	$1{\cdot}27 \times 10^{5}$	$3{\cdot}16 \times 10^{-5}$	$3{\cdot}17 \times 10^{4}$	$5{\cdot}68 \times 10^{-4}$	$1{\cdot}06 \times 10^{5}$	$3{\cdot}79 \times 10^{-5}$	$2{\cdot}64 \times 10^{4}$

TABLE A-2

COMPARISON OF MODEL PREDICTED VALUES AND EXPERIMENTAL DATA IN RAMBOID CHANGE OF SHEAR RATE

FOR BLOOD A

SHEAR RATE ($sec.^{-1}$)	SHEAR STRESS (MEASURED) ($dyne/cm^2$)		VISCOSITY (MEASURED) (poise)		SHEAR STRESS (PREDICTED) ($dyne/cm^2$)		PERCENTAGE ERROR (%)	
	UPWARD CURVE	DOWNWARD CURVE	UPWARD CURVE	DOWNWARD CURVE	UPWARD CURVE	DOWNWARD CURVE	UPWARD CURVE	DOWNWARD CURVE
2.22	0.601	0.443	0.271	0.200	0.585	0.434	2.64	1.91
3.38	0.732	0.612	0.216	0.181	0.727	0.607	0.705	0.784
4.55	0.858	0.773	0.185	0.167	0.857	0.761	0.118	1.51
5.72	0.990	0.905	0.171	0.156	0.984	0.912	0.644	0.372
6.89	1.11	1.04	0.158	0.150	1.10	1.03	0.108	1.02
8.05	1.23	1.16	0.151	0.143	1.22	1.15	0.864	0.881
9.22	1.32	1.26	0.143	0.136	1.33	1.26	-0.244	0.047
11.6	1.51	1.47	0.131	0.127	1.53	1.47	-0.944	-0.039
13.9	1.70	1.68	0.122	0.121	1.71	1.66	-0.441	1.01
16.2	1.87	1.85	0.115	0.114	1.88	1.84	-0.712	0.895
18.6	2.04	2.02	0.110	0.109	2.04	2.00	0.018	0.974
20.9	2.20	2.19	0.105	0.105	2.19	2.15	0.347	1.45
23.2	2.36	2.35	0.102	0.101	2.34	2.30	1.00	2.18
25.6	2.50	2.49	0.0979	0.0977	2.47	2.44	0.946	2.18
27.9	2.62	2.62	0.0942	0.0942	2.61	2.61	0.587	0.587

TABLE A-3

COMPARISON OF MODEL PREDICTED VALUES AND EXPERIMENTAL DATA IN RAMBOID CHANGE OF SHEAR RATE

FOR BLOOD C

SHEAR RATE ($sec.^{-1}$)	SHEAR STRESS (MEASURED) ($dyne/cm^2$)		VISCOSITY (MEASURED) (poise)		SHEAR STRESS (PREDICTED) ($dyne/cm^2$)		PERCENTAGE ERROR (%)	
	UPWARD CURVE	DOWNWARD CURVE	UPWARD CURVE	DOWNWARD CURVE	UPWARD CURVE	DOWNWARD CURVE	UPWARD CURVE	DOWNWARD CURVE
2.22	0.598	0.440	0.269	0.198	0.615	0.428	-2.86	2.68
3.38	0.776	0.610	0.229	0.180	0.752	0.599	3.08	1.71
4.55	0.907	0.775	0.195	0.167	0.874	0.753	3.59	2.87
5.72	1.03	0.913	0.178	0.157	0.993	0.892	3.89	2.31
6.89	1.11	1.04	0.164	0.149	1.11	1.02	3.11	1.42
8.05	1.25	1.16	0.153	0.143	1.22	1.14	2.00	1.98
9.22	1.35	1.25	0.145	0.135	1.33	1.25	1.43	0.081
11.6	1.52	1.44	0.131	0.124	1.52	1.46	-0.222	-1.35
13.9	1.70	1.62	0.122	0.116	1.71	1.65	-0.255	-1.60
16.2	1.86	1.80	0.114	0.111	1.87	1.82	-0.915	-1.34
18.6	2.02	1.97	0.109	0.106	2.03	1.98	-0.526	-0.429
20.9	2.17	2.14	0.104	0.103	2.18	2.13	-0.235	0.507
23.2	2.32	2.30	0.100	0.0993	2.32	2.28	-0.305	1.17
25.6	2.46	2.46	0.0964	0.0964	2.46	2.42	0.158	1.79
27.9	2.61	2.61	0.0937	0.0937	2.58	2.58	0.970	0.970

TABLE A-4

COMPARISON OF MODEL PREDICTED VALUES
AND EXPERIMENTAL DATA IN RAMBOID
CHANGE OF SHEAR RATE

FOR BLOOD D

SHEAR RATE ($sec.^{-1}$)	SHEAR STRESS (MEASURED) ($dyne/cm^2$)		VISCOSITY (MEASURED) (poise)		SHEAR STRESS (PREDICTED) ($dyne/cm^2$)		PERCENTAGE ERROR (%)	
	UPWARD CURVE	DOWNWARD CURVE	UPWARD CURVE	DOWNWARD CURVE	UPWARD CURVE	DOWNWARD CURVE	UPWARD CURVE	DOWNWARD CURVE
2.22	0.581	0.389	0.262	0.176	0.573	0.388	1.41	0.388
3.38	0.709	0.554	0.210	0.164	0.710	0.550	-0.083	0.550
4.55	0.846	0.720	0.182	0.155	0.829	0.697	2.00	0.687
5.72	0.968	0.831	0.167	0.143	0.944	0.832	2.41	0.832
6.89	1.07	0.948	0.154	0.136	1.06	0.958	1.54	0.958
8.05	1.18	1.06	0.145	0.130	1.17	1.08	1.11	1.08
9.22	1.27	1.18	0.137	0.127	1.27	1.19	0.338	1.19
11.6	1.48	1.39	0.127	0.120	1.47	1.39	0.626	1.39
13.9	1.66	1.58	0.120	0.113	1.65	1.58	0.879	1.58
16.2	1.82	1.74	0.112	0.107	1.82	1.76	-0.051	1.76
18.6	1.97	1.91	0.106	0.103	1.98	1.92	-0.019	1.92
20.9	2.12	2.07	0.102	0.0993	2.13	2.07	-0.204	2.07
23.2	2.23	2.22	0.0977	0.0961	2.27	2.22	-0.136	2.22
25.6	2.41	2.38	0.0943	0.0934	2.41	2.35	0.006	2.35
27.9	2.53	2.53	0.0910	0.0910	2.53	2.53	-0.036	-0.036

TABLE A-5

COMPARISON OF MODEL PREDICTED VALUES AND EXPERIMENTAL DATA IN RAMBOID CHANGE OF SHEAR RATE

FOR BLOOD E

SHEAR RATE ($sec.^{-1}$)	SHEAR STRESS (MEASURED) ($dyne/cm^2$)		VISCOSITY (MEASURED) (poise)		SHEAR STRESS (PREDICTED) ($dyne/cm^2$)		PERCENTAGE ERROR (%)	
	UPWARD CURVE	DOWNWARD CURVE	UPWARD CURVE	DOWNWARD CURVE	UPWARD CURVE	DOWNWARD CURVE	UPWARD CURVE	DOWNWARD CURVE
2.22	0.564	0.389	0.254	0.176	0.554	0.389	1.71	0.101
3.38	0.682	0.554	0.200	0.164	0.678	0.547	0.605	1.39
4.55	0.797	0.681	0.172	0.147	0.793	0.688	0.519	-1.05
5.72	0.918	0.820	0.158	0.141	0.906	0.818	1.35	0.260
6.89	1.02	0.937	0.147	0.135	1.02	0.937	0.807	-0.025
8.05	1.12	1.04	0.138	0.128	1.12	1.05	-0.130	-0.491
9.22	1.24	1.16	0.134	0.126	1.22	1.15	0.177	1.11
11.6	1.41	1.33	0.122	0.115	1.41	1.35	0.457	-1.11
13.9	1.58	1.50	0.113	0.108	1.58	1.52	0.069	-1.24
16.2	1.74	1.66	0.107	0.102	1.73	1.68	0.617	-1.26
18.6	1.88	1.81	0.102	0.0979	1.88	1.83	0.340	-0.849
20.9	2.03	1.97	0.0970	0.0942	2.02	1.97	0.312	-0.347
23.2	2.15	2.13	0.0928	0.0917	2.15	2.11	0.167	0.924
25.6	2.27	2.27	0.0899	0.0888	2.27	2.24	-0.361	1.35
27.9	2.38	2.38	0.0856	0.0856	2.39	2.39	-0.386	-0.386

TABLE A-6

COMPARISON OF MODEL PREDICTED VALUES
AND EXPERIMENTAL DATA IN RAMBOID
CHANGE OF SHEAR RATE

FOR BLOOD F

SHEAR RATE ($sec.^{-1}$)	SHEAR STRESS (MEASURED) ($dyne/cm^2$)		VISCOSITY (MEASURED) (poise)		SHEAR STRESS (PREDICTED) ($dyne/cm^2$)		PERCENTAGE ERROR (%)	
	UPWARD CURVE	DOWNWARD CURVE	UPWARD CURVE	DOWNWARD CURVE	UPWARD CURVE	DOWNWARD CURVE	UPWARD CURVE	DOWNWARD CURVE
2.22	0.513	0.384	0.231	0.153	0.508	0.339	1.08	-0.045
3.38	0.621	0.488	0.183	0.144	0.615	0.478	0.924	1.96
4.55	0.714	0.604	0.154	0.130	0.713	0.604	0.126	-0.006
5.72	0.815	0.722	0.140	0.124	0.811	0.720	0.392	0.223
6.89	0.910	0.825	0.131	0.119	0.907	0.827	0.284	-0.201
8.05	1.01	0.935	0.124	0.115	1.00	0.927	0.509	0.844
9.22	1.10	1.02	0.118	0.110	1.09	1.02	0.567	-0.081
11.6	1.26	1.20	0.108	0.103	1.26	1.19	-0.004	0.168
13.9	1.42	1.34	0.102	0.0962	1.41	1.35	0.517	-0.888
16.2	1.56	1.47	0.0964	0.0907	1.55	1.50	0.980	-1.63
18.6	1.70	1.62	0.0915	0.0871	1.68	1.63	1.03	-0.979
20.9	1.81	1.76	0.0841	0.0841	1.81	1.76	0.218	-0.193
23.2	1.93	1.88	0.0833	0.0812	1.92	1.88	0.438	0.249
25.6	2.03	2.00	0.0797	0.0786	2.04	1.99	-0.109	0.508
27.9	2.12	2.12	0.0763	0.0763	2.14	2.14	-0.854	-0.854

TABLE A-7

COMPARISON OF MODEL PREDICTED VALUES
AND EXPERIMENTAL DATA IN RAMBOID
CHANGE OF SHEAR RATE

FOR BLOOD W

SHEAR RATE ($sec.^{-1}$)	SHEAR STRESS (MEASURED) ($dyne/cm^2$)		VISCOSITY (MEASURED) (poise)		SHEAR STRESS (PREDICTED) ($dyne/cm^2$)		PERCENTAGE ERROR (%)	
	UPWARD CURVE	DOWNWARD CURVE	UPWARD CURVE	DOWNWARD CURVE	UPWARD CURVE	DOWNWARD CURVE	UPWARD CURVE	DOWNWARD CURVE
2.22	0.530	0.341	0.239	0.154	0.545	0.336	-2.81	1.47
3.38	0.626	0.474	0.185	0.140	0.631	0.470	-0.754	0.755
4.55	0.720	0.599	0.155	0.129	0.713	0.590	0.945	1.52
5.72	0.804	0.694	0.138	0.120	0.798	0.698	0.723	-0.565
6.89	0.872	0.790	0.125	0.114	0.883	0.798	-1.31	-0.974
8.05	0.962	0.902	0.118	0.111	0.967	0.890	-0.471	1.36
9.22	1.05	0.982	0.113	0.106	1.05	0.976	0.539	0.582
11.6	1.19	1.13	0.102	0.0970	1.20	1.13	-0.965	-0.789
13.9	1.33	1.29	0.0955	0.0923	1.33	1.28	-0.328	0.622
16.2	1.46	1.38	0.0897	0.0851	1.46	1.41	-0.224	-2.02
18.6	1.57	1.52	0.0848	0.0819	1.58	1.53	-0.234	-0.767
20.9	1.69	1.64	0.0810	0.0790	1.69	1.65	0.0780	0.168
23.2	1.80	1.77	0.0777	0.0764	1.80	1.75	0.427	0.999
25.6	1.91	1.89	0.0749	0.0742	1.90	1.86	-0.760	1.99
27.9	2.02	2.02	0.0725	0.0725	1.99	1.99	1.31	1.31

TABLE A-8

COMPARISON OF MODEL PREDICTED VALUES
AND EXPERIMENTAL DATA IN RAMBOID
CHANGE OF SHEAR RATE

FOR BLOOD Y

SHEAR RATE ($sec.^{-1}$)	SHEAR STRESS (MEASURED) ($dyne/cm^2$)		VISCOSITY (MEASURED) (poise)		SHEAR STRESS (PREDICTED) ($dyne/cm^2$)		PERCENTAGE ERROR (%)	
	UPWARD CURVE	DOWNWARD CURVE	UPWARD CURVE	DOWNWARD CURVE	UPWARD CURVE	DOWNWARD CURVE	UPWARD CURVE	DOWNWARD CURVE
2.22	0.510	0.292	0.230	0.132	0.511	0.298	-0.092	-2.02
3.38	0.549	0.405	0.162	0.120	0.563	0.411	-2.62	-1.49
4.55	0.610	0.506	0.131	0.109	0.620	0.509	-1.65	-0.755
5.72	0.672	0.590	0.116	0.102	0.684	0.598	-1.75	-1.23
6.89	0.735	0.670	0.106	0.0963	0.750	0.678	-2.02	-1.18
8.05	0.804	0.750	0.0991	0.0924	0.816	0.752	-1.40	-0.275
9.22	0.868	0.810	0.0935	0.0883	0.879	0.821	-1.24	-0.201
11.6	0.985	0.942	0.0849	0.0812	0.996	0.946	-1.13	-0.511
13.9	1.08	1.05	0.0780	0.0753	1.10	1.06	-1.62	-1.07
16.2	1.18	1.15	0.0731	0.0711	1.20	1.16	-1.24	-0.739
18.6	1.28	1.25	0.0691	0.0674	1.29	1.26	-0.933	-0.634
20.9	1.37	1.34	0.0658	0.0640	1.38	1.35	-0.638	-0.903
23.2	1.45	1.43	0.0627	0.0615	1.46	1.43	-0.753	-0.432
25.6	1.53	1.53	0.0601	0.0601	1.54	1.51	-0.554	1.29
27.9	1.64	1.64	0.0587	0.0587	1.62	1.62	1.16	1.16

TABLE A-9

COMPARISON OF MODEL PREDICTED VALUES AND EXPERIMENTAL DATA IN STEP CHANGE OF SHEAR RATE

FOR BLOOD A

TIME (sec.)	SHEAR STRESS (MEASURED) ($dyne/cm^2$)	VISCOSITY (MEASURED) (poise)	SHEAR STRESS (PREDICTED) ($dyne/cm^2$)	PERCENTAGE ERROR (%)
0.50	0.920	0.202	0.923	-0.322
0.75	0.867	0.191	0.865	0.227
1.00	0.836	0.184	0.834	0.252
1.25	0.817	0.179	0.816	0.110
1.50	0.806	0.177	0.806	0.046
1.75	0.800	0.176	0.800	-0.035
2.00	0.796	0.175	0.797	-0.160
2.50	0.795	0.175	0.794	0.067
3.00	0.794	0.174	0.794	0.052
3.50	0.794	0.174	0.793	0.090
4.00	0.794	0.174	0.793	0.102
4.50	0.794	0.174	0.793	0.106

TABLE A-10

COMPARISON OF MODEL PREDICTED VALUES AND EXPERIMENTAL DATA IN STEP CHANGE OF SHEAR RATE

FOR BLOOD C

TIME (sec.)	SHEAR STRESS (MEASURED) (dyne/cm^2)	VISCOSITY (MEASURED) (poise)	SHEAR STRESS (PREDICTED) (dyne/cm^2)	PERCENTAGE ERROR (%)
0.50	0.938	0.206	0.932	0.671
0.75	0.892	0.196	0.873	2.09
1.00	0.857	0.188	0.839	2.12
1.25	0.830	0.182	0.818	1.45
1.50	0.814	0.179	0.805	1.05
1.75	0.799	0.176	0.798	0.190
2.00	0.790	0.174	0.793	-0.300
2.50	0.784	0.172	0.788	-0.487
3.00	0.782	0.172	0.786	-0.604
3.50	0.780	0.171	0.786	-0.690
4.00	0.779	0.171	0.785	-0.831
4.50	0.778	0.170	0.785	-0.993

TABLE A-11

COMPARISON OF MODEL PREDICTED VALUES AND EXPERIMENTAL DATA IN STEP CHANGE OF SHEAR RATE

FOR BLOOD D

TIME (sec.)	SHEAR STRESS (MEASURED) (dyne/cm^2)	VISCOSITY (MEASURED) (poise)	SHEAR STRESS (PREDICTED) (dyne/cm^2)	PERCENTAGE ERROR (%)
0.50	0.852	0.187	0.849	0.367
0.75	0.803	0.176	0.808	-0.579
1.00	0.779	0.171	0.781	-0.269
1.25	0.755	0.166	0.763	-1.13
1.50	0.744	0.163	0.751	-0.995
1.75	0.736	0.162	0.743	-1.02
2.00	0.731	0.161	0.738	-0.653
2.50	0.730	0.160	0.732	-0.189
3.00	0.729	0.160	0.729	0.008
3.50	0.728	0.160	0.728	-0.001
4.00	0.728	0.160	0.727	0.080
4.50	0.728	0.160	0.727	0.117

TABLE A-12

COMPARISON OF MODEL PREDICTED VALUES AND EXPERIMENTAL DATA IN STEP CHANGE OF SHEAR RATE

FOR BLOOD E

TIME (sec.)	SHEAR STRESS (MEASURED) (dyne/cm^2)	VISCOSITY (MEASURED) (poise)	SHEAR STRESS (PREDICTED) (dyne/cm^2)	PERCENTAGE ERROR (%)
0.50	0.833	0.183	0.829	0.477
0.75	0.798	0.175	0.784	1.74
1.00	0.776	0.171	0.757	2.46
1.25	0.757	0.166	0.741	2.15
1.50	0.741	0.163	0.731	1.34
1.75	0.730	0.160	0.725	0.700
2.00	0.722	0.159	0.722	0.096
2.50	0.714	0.157	0.718	-0.527
3.00	0.712	0.156	0.717	-0.713
3.50	0.709	0.156	0.716	-1.02
4.00	0.707	0.155	0.716	-1.19
4.50	0.707	0.155	0.716	-1.18

TABLE A-13

COMPARISON OF MODEL PREDICTED VALUES AND EXPERIMENTAL DATA IN STEP CHANGE OF SHEAR RATE

FOR BLOOD F

TIME (sec.)	SHEAR STRESS (MEASURED) (dyne/cm^2)	VISCOSITY (MEASURED) (poise)	SHEAR STRESS (PREDICTED) (dyne/cm^2)	PERCENTAGE ERROR (%)
0.50	0.728	0.160	0.712	-0.561
0.75	0.693	0.152	0.695	-0.351
1.00	0.671	0.147	0.672	-0.113
1.25	0.658	0.144	0.657	0.099
1.50	0.650	0.143	0.647	0.336
1.75	0.641	0.141	0.641	0.053
2.00	0.636	0.140	0.637	-0.154
2.50	0.633	0.139	0.633	0.112
3.00	0.631	0.139	0.631	-0.017
3.50	0.629	0.138	0.630	-0.103
4.00	0.628	0.138	0.630	-0.263
4.50	0.628	0.138	0.630	-0.239

TABLE A-14

COMPARISON OF MODEL PREDICTED VALUES AND EXPERIMENTAL DATA IN STEP CHANGE OF SHEAR RATE

FOR BLOOD W

TIME (sec.)	SHEAR STRESS (MEASURED) (dyne/cm^2)	VISCOSITY (MEASURED) (poise)	SHEAR STRESS (PREDICTED) (dyne/cm^2)	PERCENTAGE ERROR (%)
0.50	0.763	0.168	0.737	3.33
0.75	0.703	0.155	0.693	1.50
1.00	0.671	0.147	0.665	0.861
1.25	0.647	0.142	0.648	-0.171
1.50	0.628	0.138	0.637	-1.42
1.75	0.625	0.137	0.630	-0.721
2.00	0.623	0.137	0.625	-0.422
2.50	0.621	0.136	0.620	0.142
3.00	0.620	0.136	0.618	0.254
3.50	0.619	0.136	0.617	0.175
4.00	0.619	0.136	0.617	0.233
4.50	0.619	0.136	0.617	0.258

TABLE A-15

COMPARISON OF MODEL PREDICTED VALUES AND EXPERIMENTAL DATA IN STEP CHANGE OF SHEAR RATE

FOR BLOOD Y

TIME (sec.)	SHEAR STRESS (MEASURED) (dyne/cm^2)	VISCOSITY (MEASURED) (poise)	SHEAR STRESS (PREDICTED) (dyne/cm^2)	PERCENTAGE ERROR (%)
0.50	0.660	0.145	0.660	0.065
0.75	0.609	0.134	0.609	-0.043
1.00	0.582	0.128	0.580	0.340
1.25	0.561	0.123	0.562	-0.298
1.50	0.547	0.120	0.552	-0.814
1.75	0.542	0.119	0.545	-0.610
2.00	0.539	0.118	0.541	-0.367
2.50	0.538	0.118	0.537	0.128
3.00	0.536	0.118	0.535	0.164
3.50	0.536	0.118	0.535	0.275
4.00	0.536	0.118	0.535	0.317
4.50	0.536	0.118	0.535	0.333

NOMENCLATURE

a,b,c	= constants in equations (2-12), (2-14), (2-18), (2-23) and (3-27)
A	= a constant in equation (2-6); a constant defined by equation (3-22)
$A_i(z)$	= one independent Airy function with argument z
B	= constants in equation (2-5) and (3-5); time coefficient of thixotropic breakdown defined by equation (2-3)
$B_i(z)$	= one independent Airy function with argument z
C	= constants in equations (2-5) and (3-23); concentration in equation (2-6)
C_1,C_2	= constants
D	= diameter, cm.
D'	= linear operator
div	= readings in X-Y recorder, inches
f	= factor for degradation rate constant induced by shear rate, $sec.^{-1}$
$F(z)$	= a function defined by equation (3-40)
g	= a constant defined by equation (3-42)
$G(z)$	= a function defined by equation (3-40)
h	= total polymer units
$H(y,t)$	= a generation function defined by equation (3-13)
I	= an integral value in equation (3-13)
II	= second invariant tensor
III	= third invariant tensor
k	= constant
k_1,k_2	= the backward and the forward rate constants respectively

k_f, k_b = specific rate constants of the forward and the backward reaction respectively

k_d, k_a = rate constants of the degradation and aggregation reaction respectively

$k_{a\ i,j}$ = rate constants for aggredation of i mer and j mer into i+j mer

k_{de} = equilibrium rate constant of degradation reaction

$k_{d\ i,j}$ = rate constants for degradation of i+j mer into i mer and j mer

k', k'', k''' = constants

K = constants in equations (2-5) and (2-11); a constant defined by equation (3-42)

K_T = torsion bar constant, dyne-cm/micron

K_1, K_2 = integration constants

L = constant defined by equation (3-7)

M = coefficient of thixotropic breakdown with shear rate

$M(t-t')$ = influence function

M_1 = monomer

M_n = polymer

$[M_1]$ = monomer concentration

$[M_n]$ = polymer concentration

m = rate of change of shear rate, $sec.^{-2}$

n = polymer units; order of plastic fluids

p = a constant

P' = linear operator

r = radius, cm

$\dot{r}$ = shear rate, $sec.^{-1}$

$\dot{r}_o$ = initial shear rate, $sec.^{-1}$

$\dot{r}_m$ = maximum shear rate, sec.$^{-1}$

R = radius of cone, cm.

R(t) = relaxation spectrum of viscosity

(RPM) = rotational speed, rev./sec.

$(RPM)_{pl}$ = rotational speed of plate, rev./sec.

$(RPM)_{shaft}$ = rotational speed of shaft, rev./cm.

$(RPM)_{tach}$ = rotational speed of tachometer, rev./sec.

t = time, sec.

t_m = time required for the shear rate to reach its maximum value in ramboid change of shear rate, sec.

t_1, t_2 = time,sec.

T = temperature, ^oK

u = a functional variable defined by equation (3-31)

U = plastic viscosity, poise

U_1, U_2 = plastic viscosity at time 1 and time 2 respectively

w = a functional variable defined by equation (3-29)

x = concentration of cells or internal structure

x_e = equilibrium structure parameter

x_m = maximum possible concentration of internal structure

x_o = initial concentration of internal structure

x_1, x_2 = concentrations of entangled and disentangled polymer units respectively

y = a real number variable

z = a time variable defined by equation (3-35)

GREEK LETTERS

α	= a constant defined by equation (3-33)
α_1, α_2	= reciprocal shear stress of Newtonian and non-Newtonian units respectively in equation (2-15)
Λ	= gearbox ratio
β	= a constant defined by equation (3-34)
β_1, β_2	= reciprocal shear rate of Newtonian and non-Newtonian units respectively.
δ	= angle of cone, degree
ΔT	= displacement of transducer, microns
$(\Delta_T)_m$	= maximum displacement of transducer, microns
$\eta_0, \eta_1, --, \eta_M$	= constants
θ	= coefficient of thixotropy in equation (2-11); viscosity deficit in equation (2-30); angle, degree
λ	= reaction constant in equation (2-16)
$\lambda_0, \lambda_1, --, \lambda_N$	= constants
μ	= viscosity, poise
μ_a	= apparent viscosity, poise
μ_n	= viscosity of n-mer
μ_0	= viscosity at zero shear rate, poise
μ_θ	= viscosity at any shear rate, poise
μ_1	= undisturbed viscosity, poise
μ_∞	= viscosity at infinite shear rate, poise
$\mu(t)$	= viscosity at current time, t, poise
π	= 3.1416
ρ	= a constant in equation (2-18)

α = a constant defined by equation (3-42)

τ = shear stress, dyne/cm^2

τ_1, τ_2 = shear stress at time 1 and time 2 respectively, dyne/cm^2

τ_y = yield stress, dyne/cm^2

ϕ = fluidity, cm·sec/g

ϕ_o = minimum fluidity, cm·sec/g

ϕ_∞ = maximum fluidity, cm·sec/g

χ_i = fraction area occupied by the ith kind of flow units

ω = angular rotation speed, radius/second

Ω = angular rotation speed, rev./second

BIBLIOGRAPHY

(1) Freundlich, H., Thixotropy, Herman et Cie, Paris (1935).

(2) Fisher, E.K., Paint Rheology, pp. 271-280 (1950).

(3) Weltmann, R.N., Ind. Eng. Chem., 40, pp. 272-280 (1948).

(4) Bauer, W.H., and E.A. Collins, "Rheology," F.R. Eirich, ed., vol. 4, chapt. 8, pp. 423-459, Academic Press, New York (1967).

(5) Fredrich, D., and Chang, T.S., "Continum Mechanics," chapt. 4, Boston, Allyn and Bacon series (1965).

(6) Green, H., Ind. Chem. Eng. Anal. Ed., 14, pp. 576-585 (1942).

(7) Green, H., and Weltmann, R.N., Ind. Eng. Chem., 15, pp. 201-206 (1943).

(8) Weltmann, R.N., J. of Applied Physics, 14, pp.343-350 (1943).

(9) Green, H., and Weltmann, R.N., Ind. Eng. Chem. Anal. Ed., 18, pp. 167-172 (1946).

(10) Weltmann, R.N., J. Colloid Sci., 17, pp. 218-226 (1953).

(11) Bird, R.B., Stewart, W.E., and Lightfoot, E.N., "Transport Phenomena," pp. 1-15, Wiley, New York (1960).

(12) Burgers, J.M., and Scott-Blair, G.W., Proc. 1st Internat. Congr. Rheol., Shevaningen, Holland (1948).

(13) Reiner, M., "Lectures on Theoretical Rheology," chapter 1, North-Holland Publishing Co., New York (1960).

(14) Brydson, J.A., "Flow Properties of Polymer Melts," pp. 3-20, Van Nostrand Reinhold Co., London (1970).

(15) Severs, E.T., "Rheology of Polymers," Reinhold, New York (1962).

(16) Juliusburger, F. and Pirquet, A., Trans. Faraday Soc., 32, pp. 445 (1936).

(17) Green, H., and Weltmann, R.N., J. of Appl. Phy., 15, pp. 414-420 (1944).

(18) Dahlgren, S-E., J. Colloid Sci., pp. 151-158 (1958).

(19) Leonard, J.T. and Hazlett, R.N., Ind. Eng. Chem. Fundamentals, 5, pp. 233-237 (1966).

(20) Goodeve, C.F. and Whitfield, G.W., Trans. Faraday Soc., 34, pp. 511-520 (1838).

(21) Goodeve, C.F., Trans. Faraday Soc., 35, pp. 342-358 (1939).

(22) Moore, F., Trans. Brit. Ceram. Soc., 58, pp. 470-492 (1959).

(23) Gabrysh, A.F., Eyring, H., Mckee,N. and Culter, I., Trans. Soc. Rheol., 5, pp. 67-84 (1961).

(24) Gabrysh, A.F., Eyring, H. and Cutler, I., J. AM. Ceram. Soc., 45, pp. 334-343 (1962).

(25) Gabrysh, A.F., Eyring, H., Shimizu, M. and Assay, J., J. Appl. Phys., 34, pp. 261-265 (1963).

(26) Ree, T. and Eyring, H., J. of Appl. Phys.m 26, pp. 793-809 (1955).

(27) Weltmann, R.N., Ind. Eng. Chem., 15, pp. 424-429 (1943).

(28) Hahn, S.J., Ree, T. and Eyring, H., NLGI Spokesman, July, pp. 129-135 (1959).

(29) Hahn, S.J., Ree, T. and Eyring, H., Ind. Eng. Chem. 51, pp. 856-859 (1959).

(30) Denny, D.A. and Brodkey, R.S., J. of Appl. Phys., 33, pp. 2269-2275 (1962).

(31) Cheng, D.C.-H. and Evans, F., Brit. J. Phys., 16(11), pp. 1599-1617 (1965).

(32) Cheng, D.C.-H., Brit. J. Appl. Phys., 17(2), pp. 253-263 (1966).

(33) Harris, J., Rheol. Acta, 6(1), pp. 6-12 (1967).

(34) Fredrickson, A.G., AICHE, May, pp. 436-441 (1970).

(35) A.M. North, "The Kinetics of Free Radical Polymerization," Pergamon, New York (1966).

(36) Ames, M.F., "Non-linear Ordinary Differential Equation in Transport Process," Academic Press, New York (1968).

(37) Davis, H.T., "Introduction to Non-linear Differential and Integral Equations," U.S. Government Printing Office, Washington, D.C. (1961).

(38) Abramowitz and Stegun, I.A., "Handbook of Mathematical Functions," U.S. Government Printing Office, Washington, D.C. (1964).

(39) Murphy, G.M., "Ordinary Differential Equation and their Solutions," Princeton, N.J., Van Nostrand (1960).

(40) Petrovsky, I.G., "Lectures on Partial Differential Equations," Translated from the Russian by A. Shenitzer (1950).

(41) Marquardt, D.W., J. Soc. Ind. App. Math., 11, pp. 431 (1963).

(42) "The Weissenberg Rheogoniometer Instruction Manual-Model R. 18," Sangamo Controls Limited, England.

(43) Van Wazer, J., "Viscosity and Flow Measurement," Inter-Science Pub. Corp. (1963).

(44) Aronson, M.H., "Viscosity Measurement and Control," Pittsburgh, Instruments Pub. Co. (1964).

(45) Lodge, A.S. "Elastic Liquids," Academic Press, New York (1964).

(46) Alfrey, T., "Mechanical Behavior of High Polymers," New York, Interscience Publishers (1948).

(47) Bergen, H.T., "Viscoelasticity; Phenomenological Aspects", New York, Academic Press (1960).

(48) Casson, N., "Rheology of Disperse Systems," Mill, C.C., ED., Pergamon, London (1959).

(49) J. Pryce-Jones, J. Oil & Color Chemists' Assoc. 26, pp. 3 (1943).

(50) Billington, E.W., Proc. Phys. Soc. LXXV, pp. 40-50 (1959).

(51) Cheng, D.C.-H., Nature, 216, pp. 1099-1100 (1967).

(52) Billington, E.W. and Huxley, A.S., J. of Colloid and Interface Sci., 22, pp. 257-268 (1966).

(53) Tullis, J.L., ED., "Blood Cells and Plasma Proteins," Academic Press Inc. (1953).

(54) Baon, W.H. and Happer, A.M., ED., "Blood Flow through Organs and Tissues," E & S Livingstone LtD., London (1968).

(55) Frey-Wyssling, Albert, ED., "Deformation and Flow Biological Systems," Amsterdam, North-Holland Pub. Co. (1952).

(56) J. Pryce-Jones, J. Oil & Color Chemicsts' Assoc. 19, pp. 295 (1936).

(57) J. Pryce-Jones, J. Sci. Inst. 18, pp. 39 (1941).

(58) Copley, A.L., Proc. 5 Internat. Congr. Rheology, ED., S. Onogim Tokyo, Univ. of Tokyo Press; Baltimore, Md. and Manchester, England, Univ. Park Press, 2, pp. 3 (1970).

(59) Chien, S., Personal Communication to A.L. Copley, Sept., 1970.

(60) Whitemore, R.L., "Rheology of the Circulation," Pergamon Press, London (1968).

(61) Dintenfass, L., "Blood Microrheology," Butterworth & Co., London (1971).

(62) Copley, A.L., Sci. 94, pp. 543 (1941).

(63) Copley, A.L. et al., J. Chem. Physiol., 26, pp. 49 (1942).

(64) Cokelet, G.R., Merrill, E.W., Gilliland, E.R. and Shin, H., Trans, Soc. Rheo. 7, pp. 303 (1963).

(65) Gilineon, P.J., Jr., Dauwalter, C.R. and Merrill, E.W., Trans. Soc. Rheol. 7, pp. 319 (1963).

(66) King, R.G. and Copley, A.L., Biorheology, 7, pp. 1 (1970).

(67) Rutgers, R., Rheol. Acta, 2, pp. 201-210 (1962).

(68) Haynes, R.H. and Burton, A.C., Am. J. Physiol., 197, pp. 943-950 (1959).

(69) Azuma, T., Biorheol., 2, pp. 159-160 (1964).

(70) Bugliarello, G. and Hayden, J.W., Trans. Soc. Rheol., 7, pp. 209-230 (1963).

(71) Wells, R., Schmid-Schoenbein, H. and Goldstone, J., "Theoretical and Clinical Homorheology," Proc. 2nd Internal. Conference.

(72) Dintenfall, L., Rheol. Acta, 2, pp. 187 (1962).

(73) Fredrickson, A.G., "Principles and Applications of Rheology," Prentice-Hall, Englewood Cliffs, N.J. (1964).

(74) Billmeyer, F.W. Jr., "Textbook of Polymer Science," John Willey and Sons, Inc. (1971).

(75) Tanford, C., "Physical Chemistry of Macromolecules," New York, Wiley (1961).

(76) Billington, E.W., Proc. Phys. Soc. (London), 75, pp. 40-50 (1960).

(77) Billington, E.W., Proc. Phys. Soc. (London), 76, pp. 127-136 (1960).

(78) Billinton, E.W., J. Sci. Instr., 42, pp. 569-575 (1965).

(79) Billington, E.W. and Huxley, A.S. J. of Colloid and Interface Sci., 22, pp. 257-268 (1966).

(80) Gabrysh, A.F., Eyring, H, Ma, S. -M. and Liang, K., The Review of Scientific Instr. 33(6), pp. 670-682 (1962).

(81) Savins, J.G., Rheologica Acta, 7, pp. 87-93 (1968).